Group IV Nanoparticles: Synthesis, Properties, and Biological Applications

Jiyang Fan and Paul K. Chu**

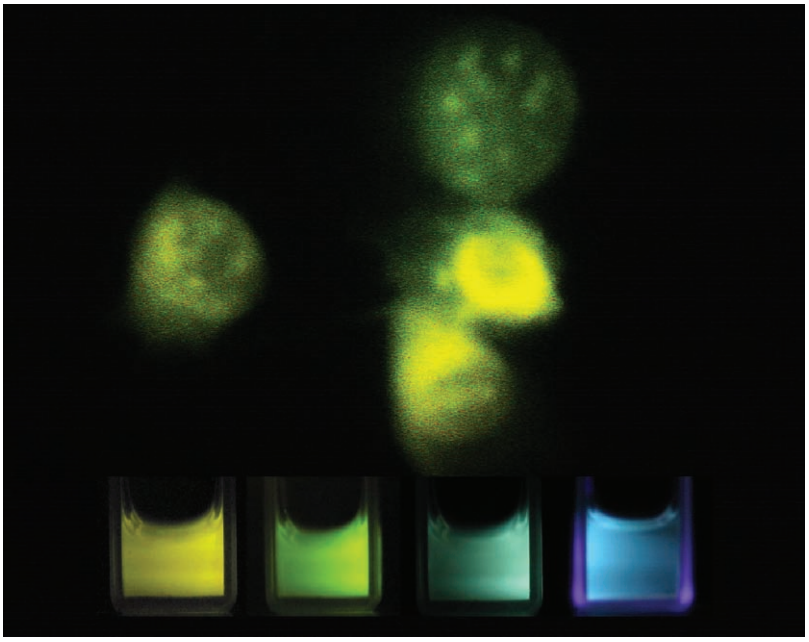

From the Contents

In this review, the emerging roles of group IV nanoparticles including silicon, diamond, silicon carbide, and germanium are summarized and discussed from the perspective of biologists, engineers, and medical practitioners. The synthesis, properties, and biological applications of these new nanomaterials have attracted great interest in the past few years. They have gradually evolved into promising biomaterials due to their innate biocompatibility; toxic ions are not released when they are used in vitro or in vivo, and their wide fluorescence spectral regions span the near-infrared, visible, and near-ultraviolet ranges. Additionally, they generally have good resistance against photobleaching and have lifetimes on the order of nanoseconds to microseconds, which are suitable for bioimaging. Some of the materials possess unique mechanical, chemical, or physical properties, such as ultrachemical and thermal stability, high hardness, high photostability, and no blinking. Recent data have revealed the superiority of these nanoparticles in biological imaging and drug delivery.

© 2010 Wiley-VCH Verlag GmbH & Co. KGaA, Weinheim

small NANO MICRO

1. Introduction

Group IV elements play crucial roles both in our daily life and in our bodies. Carbon is the backbone of all known life-forms on earth. In the human body, it is the second most abundant element by mass after oxygen. Carbon in nature exists mostly in the form of graphite, diamond, and amorphous carbon. Silicon is the basic material used in integrated circuits and the principal component of semiconductor devices. Silicon is also an essential element to sustain life. The compound of silicon and carbon, silicon carbide, a semiconductor with superior characteristics, is widely used in high-temperature, high-power, and high-frequency electronic applications. It is also one of the best biocompatible materials. The third element in this group, germanium, is also an important semiconductor and used progressively more in strained devices involving a combination of silicon and germanium.

Although group IV semiconductors are commonly found in microelectronics, they are not as popular in optics and optoelectronics. The reason lies in their indirect bandgaps, which make their luminescence efficiency very low at room temperature. In optoelectronics, devices made of group III–V compound semiconductors such as GaAs dominate at the present time.

With the advent of nanoscience and nanotechnology, there has been increasing interest in obtaining efficient luminescence from group IV nanostructures for two reasons. First of all, extensive investigations have demonstrated that the fluorescence efficiency in group IV nanostructures can be improved by several orders of magnitude with respect to that of bulk materials. Their quantum yield can be closer to or even higher than those of some bulk or nanostructured direct-bandgap semiconductors. This results from substantially enhanced radiative recombination rates and suppressed or relatively reduced nonradiative recombination rates due to spatial confinement in the nanostructures.[1] Secondly, group IV nanoparticles are more benign to human beings and environments compared with semiconductor nanocrystals that contain cytotoxic heavy metal atoms. Thirdly, fluorescent semiconductor (including group IV) nanocrystals, also known as quantum dots, have demonstrated their great potential in biological imaging and diagnostics as they have such virtues superior to traditional organic dyes as high resistance against photobleaching, composition/size-dependent absorption and emission, as well as broad absorption spectra and narrow emission spectra (for monodisperse nanoparticles).[2,3] Hence, they are suitable for long-term and multicolor labeling in the monitoring of intracellular processes.[4–6] Furthermore, they can serve as drug delivery platforms in therapeutics. Biologists have preliminarily but extensively adopted group II–VI quantum dots in various kinds of experiments, especially in bioimaging and disease diagnostics.[7,8] One major reason is that there have been relatively mature methods for synthesizing size controllable, monodisperse pure or core/shell group II–VI quantum dots that have bright fluorescence especially by chemical solution methods.[9,10] However, general group II–VI (such as CdSe) quantum dots contain heavy metal elements that are toxic to living cells and tissues.[11–13] Hence the health concern has stifled their wider biological usages especially in vivo and the task to identify substitute benign nanoparticles has become a focus in this field.[14] In this respect, group IV nanoparticles bring new hopes as benign materials accompanied by the above-mentioned properties, which favor their biological applications.

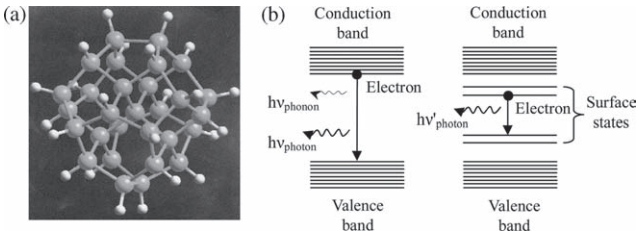

Figure 1. a) Prototype structures of $Si_{29}H_{24}$, illustrating the general diamond (or zinc blende) structure of group IV semiconductor nanocrystals. In the particle, five Si atoms constitute a single tetrahedral core and 24 Si atoms constitute a H-terminated reconstructed surface. Reproduced with permission.[33] Copyright 2002, American Institute of Physics. b) Schematic energy diagrams of a quantum dot with or without surface-related (or interior defect) traps showing distinct luminescence mechanisms. They depict the recombination processes of electrons along with the emission of photons. A phonon is simultaneously emitted in the case of an indirect semiconductor so as to maintain the conservation of momentum.

Diamond and diamondlike carbon (DLC) are used in biomedical implants and preliminary studies have also demonstrated the biocompatibility of bulk silicon.[15] Silicon carbide has also been long recognized as one of the best biocompatible materials,[16] especially in cardiovascular and blood-contacting implants and biomedical devices. Although germanium is relatively less investigated, no significant cytotoxicity of them has heretofore been observed. All these group IV materials have the face-centered cubic (diamond or zinc blende) or hexagonal covalently bonded crystal structures (**Figure 1**a). As a result, they can form chemical bonds with various types of ligands especially biomolecules.[17] Another advantage of group IV nanostructures is that they can be readily made water-soluble as-prepared or via subsequent surface functionalization; this is a necessary condition for applications in a physiological environment. The bandgaps of group IV semiconductors at room temperature are 1.12 eV for Si, 5.50 eV for diamond, and 0.66 eV for Ge, whereas diverse for SiC because it exists in over 200 crystalline forms and among them the most common types are 3C, 6H, and 4H, which have bandgaps of 2.2, 3.02, and 3.20 eV, respectively.[18] According to the quantum confinement effect, as the size of a semiconductor particle diminishes to be near or smaller than its bulk exciton Bohr diameter, the corresponding energy gap will

Prof. J. Y. Fan
Department of Physics
Southeast University
Nanjing 211189, PR China
E-mail: jyfan@seu.edu.cn
Prof. J. Y. Fan, Prof. P. K. Chu
Department of Physics and Materials Science
City University of Hong Kong
Kowloon, Hong Kong, PR China
E-mail: paul.chu@cityu.edu.hk

DOI: 10.1002/smll.201000543

 © 2010 Wiley-VCH Verlag GmbH & Co. KGaA, Weinheim

increase with decreasing size, and accordingly its fluorescence arising from interband transitions of carriers (electrons and holes) will shift to blue. As a result, the emissions in group IV nanoparticles with different sizes will span the whole spectral region from near-IR to visible to near-UV. This virtue is favorable for their applications in biological imaging and sensing.

In the following sections, we shall summarize the achievements in group IV nanoparticles involving their synthesis, properties, and various biological applications. To make the clues clearer, we shall discuss each kind of the semiconductor quantum dot one by one first and then give a discussion on the similarities and differences among them.

Jiyang Fan received his BS in physics from Shandong University in 1996, and a MS in theoretical physics from the Institute of Theoretical Physics at Chinese Academy of Sciences in 2001. He received his PhD in condensed matter physics majoring in nanoscience and nanotechnology at Nanjing University in 2006. In 2007 he joined the faculty of Southeast University, where he is now an associate professor of physics. His research mainly concerns the structural, optical, and electrical properties of semiconductor nanomaterials and also works to develop their biological applications.

Paul K. Chu received his BS in mathematics from The Ohio State University in 1977, and MS and PhD in chemistry from Cornell University in 1979 and 1982, respectively. He is a Chair Professor of Materials Engineering at the City University of Hong Kong. His research activities are quite diverse encompassing plasma surface engineering and various types of materials and nanotechnology. Paul has co-authored 800 journal papers, 6 books, and 15 patents. He is a senior editor of *IEEE Trans. Plasma Sci.* and associate editor of *Mater. Sci. Eng. R* and *Int. J. Plasma Sci. Eng*. He has won a number of awards including the 2007 IEEE NPSS Merit Award.

2. Mechanisms of Light Emission

The characteristics of the emission from a semiconductor nanoparticle that are closely associated with their biological applications mainly contain peak wavelength, full width at half maximum (FWHM), quantum yield, lifetime, and photostability. All of these features are strongly dependent on the luminescence mechanism of the nanoparticle. The direct-bandgap group II–VI quantum dots generally show very simple luminescence mechanism with their fluorescence originating from interband transitions of carriers. In contrast, the emissions from group IV nanoparticles can be much more complex, and they depend not only on the semiconductor type, but also on the specific fabrication method because it can result in distinct interior defects as well as surface reconstruction and bonding structures. The environment can also play a key role in determining the luminescence properties of some types of group IV nanoparticles. Similar to case of group II–VI quantum dots, the emissions in group IV nanoparticles may also stem from interband transitions of carriers (Figure 1b). In this circumstance, the emissions obey the quantum confinement effect and will monotonically shift to blue with decreasing particle size. On the other hand, the interior defects such as vacancies and substitutional impurities as well as the surface defects may serve as capturing centers of carriers in some nanoparticles, thereby resulting in correlated luminescence. The peak wavelength of such defect-related luminescence generally depends only weakly on particle size. To enhance the photostability of the nanoparticles as well as to improve their quantum yields, some measures have been taken which include encapsulation of the nanoparticles with oxide layers or surface passivation by specific ligands. For the luminescence originating from the defects, its brightness can be improved by increasing the defect concentration during the synthesis process of the nanoparticles. We shall discuss the respective luminescence mechanism for each kind of group IV nanoparticle in the following sections.

3. Silicon

3.1. Fabrication and Luminescence Properties

Since the discovery of room-temperature, visible strong photoluminescence in porous silicon prepared via electrochemical etching of bulk silicon,[19] there have been extensive studies on its fabrication and luminescence properties.[20,21] Its luminescence mechanisms remain controversial, and most generally accepted ones are quantum confinement effects and surface states.[19,22–24] In general, the surface of freshly prepared porous silicon is primarily terminated by hydrogen, and it exhibits luminescence originating from the quantum confinement effect, but after storage in air for a few minutes or seconds the sample will be oxidized resulting in surfaces states-related luminescence. However, in most cases, it is difficult to identify the specific luminescence mechanism from the spectral features and in some cases quantum confinement and surface states can even contribute simultaneously. Sometimes, the adsorption of specific molecules to a porous Si can result in quenching of its emissions owing to the energy transfer between them and following this principle a variety of chemical sensors can be made.[25]

In the past decade, silicon nanocrystals have gradually replaced porous silicon to become the research focus.[26] Similar to porous Si, the luminescence mechanism of Si nanocrystals is complex arising from both quantum confinement and surface defect states.[27,28] In addition to the generally observed single exciton generation upon absorption of a photon in Si nanocrystals, the multiple exciton generation upon absorption of a single photon as well as one photon emission under multiphoton excitation has also been observed.[29,30] All of these types of the luminescence have their special applications in biological imaging.

A variety of methods have been developed to fabricate freestanding silicon nanoparticles. Electrochemical etching

© 2010 Wiley-VCH Verlag GmbH & Co. KGaA, Weinheim

small NANO MICRO

of bulk Si combined with sonication is a proven method to produce luminescent Si crystallites with size of some micrometers to nanometers.[31–35] Pyrolysis of silane by laser heating, microdischarge, microwave, and plasma treatment under different conditions has also been used to synthesize luminescent Si nanocrystals possessing different dimensions.[36–47] Laser ablation of a silicon target in unsaturated 1-alkene generates 1-alkene-capped 1–10 nm blue/UV luminescent Si nanocrystals.[48] Silicon nanocrystals with average diameters of 1–5 nm can be synthesized by thermal vaporization of Si followed by exposure to atomic hydrogen to passivate the surface.[49] The solution route constitutes another series of methods to fabricate Si nanocrystals. Wet chemistry approaches such as sodium naphthalenide reduction of silicon halides,[50] solution reaction of sodium silicide and ammonium bromide using standard Schlenk techniques,[51] and reaction between Br_2 and Mg_2Si powder[52] have separately yielded blue/UV luminescent colloidal Si nanocrystals with surfaces easy to functionalize. Solution-phase reduction of $SiCl_4$ with $LiAlH_4$ or with sodium naphthalenide in inverse micelles generates blue/UV luminescent colloidal Si nanocrystals with sizes of 1–10 nm depending on the experimental conditions.[53–57] Thermal degradation of diphenylsilane yields luminescent Si nanocrystals 1.5–4.0 nm in diameter with the peak wavelength varying from blue-green to near-UV depending on the average particle size. The overall quantum yield is determined to be as high as 23%.[58,59] Ultrasound-assisted electrochemical octyltrichlorosilane reduction produces blue luminescent octane-terminated Si nanocrystals with the majority particle sizes smaller than 5 nm.[60] High-energy mechanical ball milling of nonspherical millimeter-sized pieces of semiconductor-grade silicon in either alkene or alkyne produces blue luminescent alkyl/alkenyl-passivated Si crystallites containing some particles smaller than 4 nm in diameter.[61]

Many freshly prepared Si nanocrystals are hydrogen-terminated and need to be functionalized to render them hydrophilic or at least amphiphilic as well as to protect them from oxidation.[55] Hydrogen-termination is suitable for subsequent surface functionalization in that such pristine surface can readily react with alkane, alkene, or alkyne groups to produce Si–C bonds via UV irradiation, sonication, or catalysis.[42,62–65] The surface of Si nanocrystals can also be chloride terminated prior to functionalization.[50,66] Direct alkylation of a fresh silicon surface without the assistance of a hydrogen-terminated intermediate has been reported.[61] Ab initio calculations indicate that alkyl passivation only weakly affects the optical gap of silicon quantum dots and may nonlinearly enhance absorption.[67,68] However, alkyl-terminated Si nanocrystals are hydrophobic and are not preferred in biological applications in the physiological environment. Hydrophilic surface functionalization of Si nanocrystals has been achieved by using hydrophilic biocompatible organic ligands such as carboxyl,[42,69,70] amino,[54] and hydroxyl groups.[71]

3.2. Bioimaging

Si nanocrystals have several features making them suitable for biological labels. First of all, the surface of Si nanocrystals is reactive and easy to functionalize with versatile biocompatible ligands. Secondly, silicon is generally benign to cells and tissues, as verified by experiments such as cell tracking with intracellular polysilicon barcodes,[72] intracellular silicon chips,[73] and silicon electronics on silk for bioresorbable implantable devices.[74] Thirdly, Si nanocrystals may have a very high quantum yield. It has been reported that Si nanocrystals prepared by decomposition of silane followed by surface passivation with alkenes or alkynes show a quantum yield as high as 0.6 at 789 nm.[75]

By use of two photoinduced reactions followed by DNA labeling and formation of carboxamide, 1–2 nm diameter Si nanoparticles can be conjugated to a 5′-amino-modified oligonucleotide that contained a C6 linker between amide and phosphate groups in aqueous solution.[76] The oligonucleotide-conjugated nanoparticles show photoluminescence peaks at 400 and 450 nm with a quantum yield of 0.08. Alkane-terminated Si nanoparticles can also be linked to diazirine succinimidyl ester. The open end reacted with carboxyl moieties of streptavidin and formed an amide bond.[77] The streptavidin molecules retain their binding capability to biotin after conjugation.

Alkyl-capped Si nanoparticles can retain most of their photoluminescence properties in the physiological environment,[78] but their low water-solubility hampers many biological applications. Various types of organic molecules are employed to cap the surface of Si nanoparticles via covalent bond. Water-soluble luminescent poly(acrylic acid) grafted Si nanoparticles with a diameter less than 10 nm and quantum yield of 0.24 have been used for bioimaging in CHO cells.[79] The coated Si nanoparticles-labeled CHO cells show no obvious changes in luminescence intensity over a span of 2 h. Poly(acrylic acid) terminated Si nanospheres with a diameter of 70 nm can be synthesized by magnetic stirring of hydrogen-terminated Si quantum dots in an acrylic acid and ethanol solution followed by blue and successive UV irradiation.[80] Each nanosphere is composed of primary Si nanocrystals with the outermost layer composed of carboxyl groups. The nanospheres have a quantum yield of 15–20% and are useful fluorophores to label HEK293T human kidney cells. Si nanospheres generated by thermally oxidizing 35.1 nm Si nanospheres occupy a carboxyl-group outside layer with a higher quantum yield of 25%.[81] The carboxylic acid group in the oxidized Si nanospheres can readily react with the amino group of proteins to produce nanosphere/IgG conjugates that can be used in immunofluorescent imaging of human embryonic kidney cell line 293. Cytotoxicity tests by monitoring the reduction activity of methyl thiazolyl tetrazolium (MTT) show that both Si nanospheres and oxidized Si nanospheres have good biocompatibility.

The amino group is another species that can be grafted to Si nanoparticles to render them water soluble and biocompatible. Allylamine-grafted and blue luminescent Si nanocrystals 1–4 nm in diameter have been used for biological imaging in HeLa and Vero cells.[55,56] By tuning the alkyl chain length between the core nanoparticle and the amine-end group, the amine-terminated 1.57-nm Si nanoparticles exhibit tunable emissions from blue to UV.[82] The emissions are exceptionally stable over a wide pH range of 1 to 13. These capped nanoparticles

 © 2010 Wiley-VCH Verlag GmbH & Co. KGaA, Weinheim

are used in BV2 cells imaging, and appear to relocate to the newly formed cells as confirmed by proliferation of the stained cells indicating their good biocompatibility. Preparation of octadecene, ethyl undecylenate, or styrene-functionalized Si quantum dots encapsulated in amine-functionalized phospholipid micelles has also been reported (**Figure 2**a,b).[83] The encapsulated nanoparticles which have diameters of 50–120 nm and luminescence quantum yield of 2–4% show robust uptake by human pancreatic cancer cells in vitro with no sign of morphological damage to the cells (Figure 2c). The MTS assay shows an average cell viability of 85% after 48 h of co-incubation at a concentration of 8 μg mL^{-1}.

Si particles may also be used in hyperpolarized magnetic resonance imaging.[84] The Si particles adopted in the study span four orders of magnitude in diameter from 40 nm to 1 mm and exhibit remarkably long nuclear spin relaxation time ranging from many minutes to hours. They are aminated with (3-aminopropyl)triethoxysilane and then coated with polyethylene glycol (PEG). The materials show good stability and biocompatibility. The detail of application of nanoparticles in magnetic resonance imaging has been described in some comprehensive reviews.[85,86]

3.3. Cytotoxicity

The toxicity or biocompatibility is the first concern when nanoparticles are used in life sciences in vivo. The primary rat hepatocytes cell viability on nanoporous silicon approaches that found on tissue culture polystyrene.[87] Examination of the cytotoxic and inflammatory responses to luminescent 3-nm Si nanoparticles with micrometer-sized silicon particles in RAW 264.7 macrophages reveals that endotoxin-free Si nanoparticles can slightly reduce the cell viability at concentrations exceeding 20 μg mL^{-1}.[88] However, in contrast to micrometer-sized particles, no inflammatory responses can be detected from experiments involving nanoparticles up to 200 μg mL^{-1}. Passively oxidized 6.5-nm Si quantum dots that emit green light have been used in living HeLa cell imaging.[89] The toxicity of Si quantum dots is not observed at a concentration of 112 μg mL^{-1}. They show less toxicity than CdSe quantum dots at high concentrations in mitochondrial assays and with lactate dehydrogenase assays. Under UV exposure, Si quantum dots are over ten times safer than CdSe quantum dots. 1 μm Si particles prepared by milling of porous Si are observed to have a mild negative effect on the evolution of cells at very high concentrations (more than 5 μg mL^{-1} of nutrient media), but the cells are viable and cell division proceeds normally and the next cell generation shows normal behavior.[90] No internalization but only concentration on the cell membranes has been observed for these Si particles. Alkyl-capped silicon nanocrystals have been reported to induce a higher rate and extent of intracellular accumulation in human cancerous cells compared to human noncancerous primary cells.[91] The uptake of the nanocrystals by cells is primarily through cholesterol-dependent endocytosis. They show no evidence of in vitro cytotoxicity when assessed by cell morphology, apoptosis, and cell viability assays.

3.4. Drug Delivery

Porous Si particles have numerous pores that can accommodate drugs and thus have great potential as drug delivery agents.[92] Porous Si microparticles with pore size of 20–100 nm produced by electrochemical etching of bulk Si have been demonstrated to carry fluorescein isothiocyanate (FITC)-insulin, a model hydrophilic pharmacologically active protein, along with sodium laurate (C12) as the permeation enhancer to cross intestinal Caco-2 cell monolayers.[93] The ability to cross the cell monolayers with FITC-insulin loaded by silicon is enhanced by nearly 10 times compared to liquid formulations with permeation enhancers. The 126 nm porous Si particles with the pore size of 5–10 nm exhibiting near-IR emission are produced by electrochemical etching combined with ultrasonication.[94] The materials can self-destruct in the physiological environment into renally cleared components via hydrolysis of surface silicon dioxide into orthosilicic acid [$Si(OH)_4$], which is naturally found in many tissues and can be efficiently excreted from the body through urine (**Figure 3**a–c). In vivo imaging of mouse tumors and other organs using the silicon nanoparticles has also been demonstrated. The nanoparticles injected

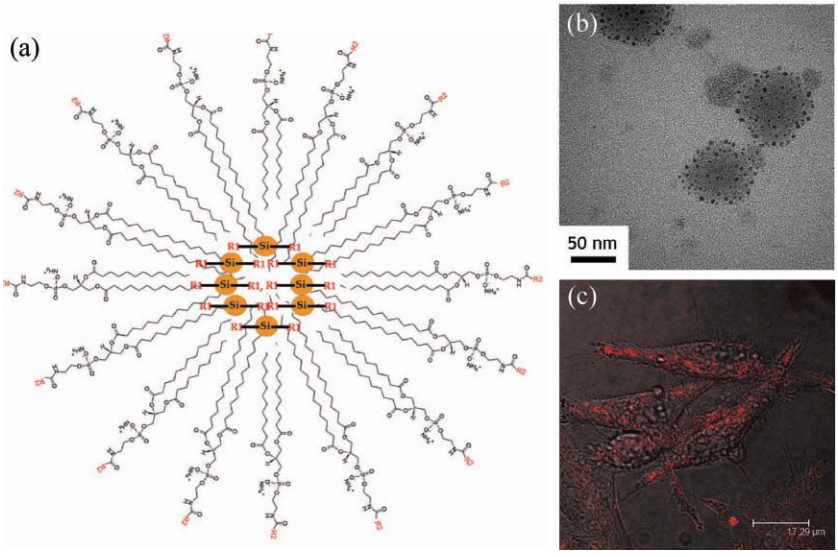

Figure 2. a) Schematic of surface functionalization of silicon quantum dots with compounds R1 (styrene, octadecene, or ethyl undecylenate) followed by encapsulation with phospholipid micelles that were terminated by the functional groups R2 (methoxy PEG, carboxyl, folate, or biotin). b) TEM images of Si quantum dots encapsulated in several micelles. c) Overlay of the confocal microscopic bright-field and fluorescence images of live pancreatic cancer cells treated with amine-terminated micelle encapsulated Si quantum dots. The scale bar is 17.29 μm. Reproduced with permission.[83] Copyright 2008, American Chemical Society.

© 2010 Wiley-VCH Verlag GmbH & Co. KGaA, Weinheim

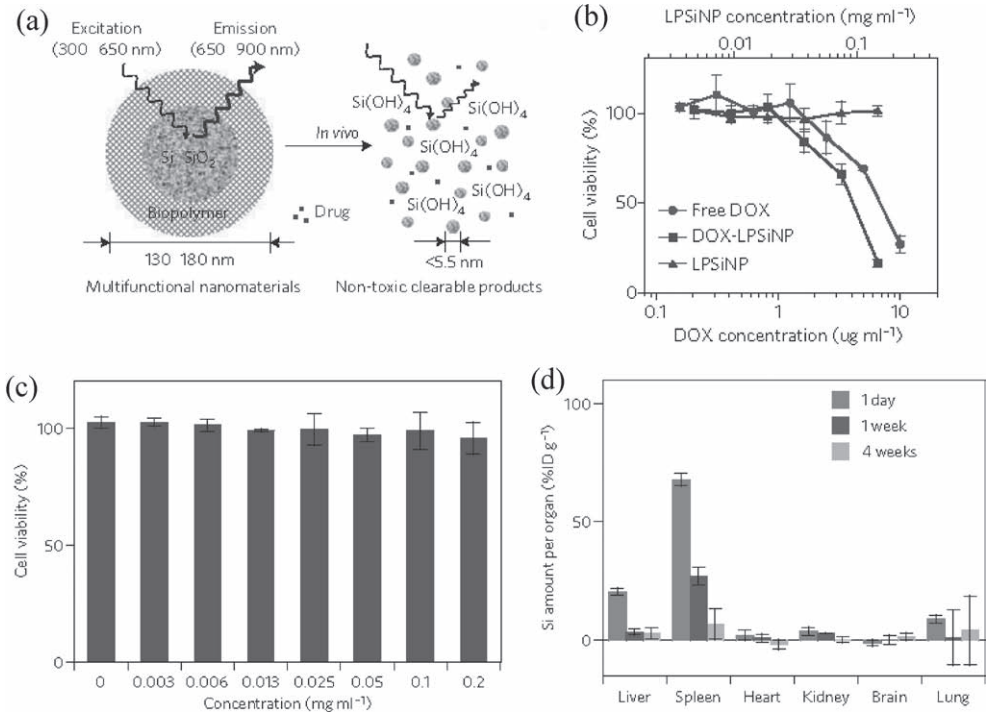

Figure 3. Characterization of luminescent porous Si nanoparticles (LPSiNP). a) Schematic diagram depicting the structure and in vivo degradation process for the biopolymer-coated nanoparticles used in this study. b) Cytotoxicity of doxorubicin (DOX)-Si nanoparticles, bare Si nanoparticles and free DOX towards MDA-MB-435 human carcinoma cells, quantified by the MTT assay. The cells were incubated with the samples for 48 h. The error bars indicate the standard deviation. c) In vitro cytotoxicity of Si nanoparticles towards HeLa cells after incubation with cells for 48 h, determined by the calcein assay. d) In vivo biodistribution and biodegradation of Si nanoparticles over a period of 4 weeks in a mouse. They were intravenously injected into the mouse (n = 3 or 4, dose = 20 mg kg^{-1}). The silicon concentration in the organs was determined at different time points after injection. Reproduced with permission.[94] Copyright 2009, Nature Publishing Group.

intravenously are observed to accumulate mainly in mononuclear phagocytic-system-related organs, degrade in vivo within a few days, and be removed from the body (Figure 3d).

4. Carbon

4.1. Fabrication and Luminescence Properties

Luminescent carbon nanoparticles can have the diamond, graphite, or mixed diamond/graphite structure. Graphite consists of parallel atomic layers. In each layer, the carbon atoms (sp^2) are arranged in a hexagonal lattice. The diamond lattice consists of tetrahedrally bonded carbon atoms (sp^3) in a face-centered cubic structure. Graphite is very soft and has good electrical conductivity, and it is opaque and black. Diamond has high hardness and is a highly transparent insulator, except blue diamond which is a semiconductor due to incorporated boron. Both graphite and diamond are highly stable and require a high temperature to react even with oxygen.

4.1.1. Diamond Nanoparticles

The static high-pressure high-temperature (HPHT) method is commonly used to produce luminescent diamond nanoparticles for biological applications. It consists of two steps with diamond crystals with diameters of tens of micrometers created first and then they are mechanically milled to produce nanodiamond. Using high energy ball milling, fluorescent HPHT diamond microcrystals are converted into isolated ultrasmall quasi-spherical diamond nanoparticles with dimensions smaller than or equal to 10 nm.[95] By means of ultracentrifugation, size-tunable isolated diamond nanoparticles with a median diameter between 4 and 25 nm are produced from primary HPHT diamond.[96] Detonation of trinitrotoluene and hexogen explosives is another method to produce nanodiamonds. In this technique, 100–200 nm aggregates composed of 4–5 nm diameter diamond nanoparticles are produced. These tight aggregates can form larger loosely aggregated agglomerates with a size of several or tens of micrometers. The primary 4–5 nm diamond nanoparticles can be liberated by stirred-media milling with micrometer-sized ceramic beads and then dispersed in polar solvents such as alcohols or in hydrocarbons in the presence of dispersing agents.[97,98] The primary detonation nanodiamond has a crystalline core and an outer shell composed of possibly amorphous carbon or disordered graphite mixed with metal particles, but the exact structure is still debatable.[99] Oxidation at 400–430 °C in air selectively removes sp^2-bonded carbon in the outer layer of the diamond nanoparticles or in the region between the aggregated particles because at this temperature, almost no oxidation of sp^3-bonded carbon occurs (**Figure 4**).[100] Atomic hydrogen treatment at a high temperature can also remove the outer

 © 2010 Wiley-VCH Verlag GmbH & Co. KGaA, Weinheim

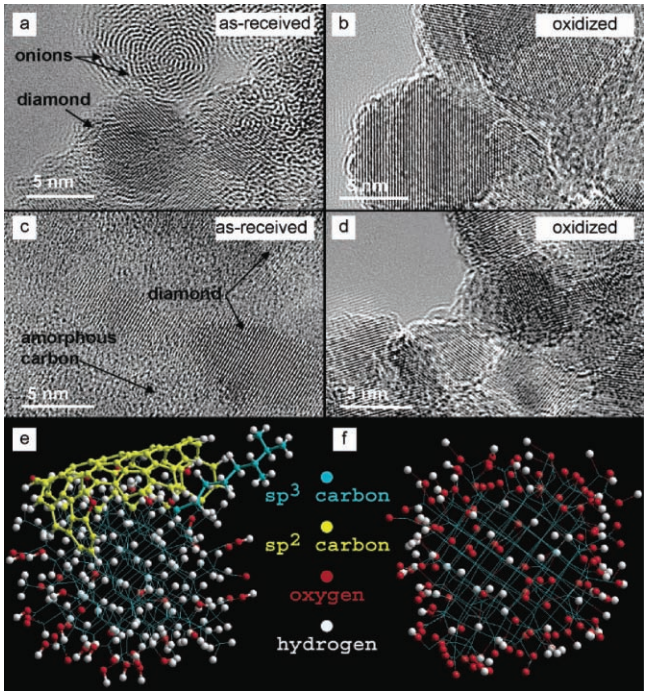

Figure 4. HRTEM images of two nanodiamond samples before and after oxidation at 425 °C for 5 h in air. The sample in a and b is the raw detonation soot containing nondiamond carbon structures such as amorphous carbon, carbon onions, fullerenic shells, and graphite ribbons. The sample in c and d was prepared by multistage acidic purifications using nitric and sulfuric acids and mainly consists of nanodiamond particles and amorphous carbon. HyperChem models of nanodiamond e) before and f) after oxidation. In addition to sp^2 carbon, all powders contain metal impurities surrounded by carbon shells. Reproduced with permission.[100] Copyright 2006, American Chemical Society.

graphitic layers resulting in hydrogen-terminated diamond nanocrystallites.[101]

Since diamond has a very wide bandgap, only defect state-related fluorescence can lie in the visible region. The most well-known color center in diamond is the nitrogen-vacancy (N-V) complex[102] formed by electron, proton, or ion irradiation followed by annealing at about 700–900 °C. Nearly all natural and synthetic diamond contains some nitrogen and irradiation creates vacancies in diamond leading to the formation of red luminescent N-V defect centers during annealing. Such defects possess some nice luminescence properties including high stability and high quantum efficiency (close to 1). Stimulated emission depletion microscopy has been used to detect fluorescent N-V centers in diamond.[103] Photon correlation spectroscopy combined with Monte Carlo simulation shows that in fluorescent 28 nm nanodiamond prepared by 3 MeV proton irradiation, there are about 8 negatively charged N-V centers per particle.[104] Near-field microscopy and photon statistics measurements show that HPHT nanodiamonds with sizes down to 25 nm can hold a single N-V color center while retaining bright and stable emission.[105]

It is difficult to prepare luminescent HPHT diamond particles smaller than 10 nm. Density functional simulation suggests that both nitrogen and boron are metastable in the nanodiamond core.[106] Some progress has recently been made. Time-gated luminescence reveals the existence of both neutral and negative N-V centers in weakly bound clusters containing 5 nm nanodiamonds produced by proton-irradiation.[107] A method based on micronization and nanomilling converts as-grown HPHT diamond microcrystals into spatially isolated N-V-rich diamond nanoparticles with sizes of or smaller than 10 nm showing stable fluorescence without photobleaching.[95] Stable emission has also been achieved from N-V centers in isolated nanodiamonds with a mean size of 8 nm.[108]

Compared to HPHT nanodiamonds little is known about the position and distribution of nitrogen in detonation nanodiamonds which have much smaller sizes. Electron energy loss spectroscopy (EELS) combined with model-based quantification provides direct evidence on sp^3 like embedding of nitrogen impurities in the diamond core.[109] The atomic nitrogen concentration is 3 at% in half of the primary diamond particles with sizes smaller than 6 nm.[110] Only particles larger than 30 nm exhibit photoluminescence arising from the N-V centers.

Besides N-V centers in HPHT and detonation nanodiamonds, several other methods have also been employed to produce luminescent nanodiamonds. Chemical vapor deposition using methane and hydrogen generates diamond nanocrystals, among which those particles larger than 40 nm exhibit N-V emissions.[111] The 2–5 nm diamond nanocrystals produced by microwave plasma deposition show fluorescence at 738 and 757 nm originating from silicon-vacancy centers.[112] Nickel-nitrogen defect centers created in diamond give rise to a narrow emission spectrum at 797 nm.[113] Laser irradiation of carbon black or graphite powder in water produces diamond nanocrystals with most probable diameters of 3.6 and 4.0 nm which emit at 510 and 505 nm, respectively, after surface passivation with poly(ethylene glycol) or diamine-terminated oligomeric poly(ethylene glycol).[114–116] A recent work indicates that two photon excitation (at 1064 nm) can result in emissions from negatively charged N-V centers in type Ib diamond single crystals with the spectral features and fluorescence lifetime almost the same as those of one-photon excitation.[117] Such IR excitation has the virtue of long penetration depth through biological tissues.

Surface treatment of freshly prepared diamond nanoparticles is difficult due to their complex surface structures. Treatment of detonation diamond agglomerates composed of primary 3.5–6.5 nm diamond particles is conducted using a mixture of fluorine and hydrogen gases at 150–470 °C.[118] The fluoro-nanodiamond forms alkyl-, amino-, and amino-acid-nanodiamond derivatives and the solubility in polar organic solvents is improved while the agglomerate size diminishes from several micrometers to tens of nanometers. Oxidation in air leads to surface functionization on detonation diamond nanoparticles yielding oxygen-containing carboxyl or hydroxyl functional groups.[100] Chemical modification of ultradispersed nanodiamond is demonstrated to enrich the surface hydroxyl groups which can be readily functionalized with long chain alcohols.[119] By means of the Suzuki coupling reactions, nanodiamonds can be functionalized with trifluoroaryls to yield improved solubility in ethanol and hexane.[120]

© 2010 Wiley-VCH Verlag GmbH & Co. KGaA, Weinheim

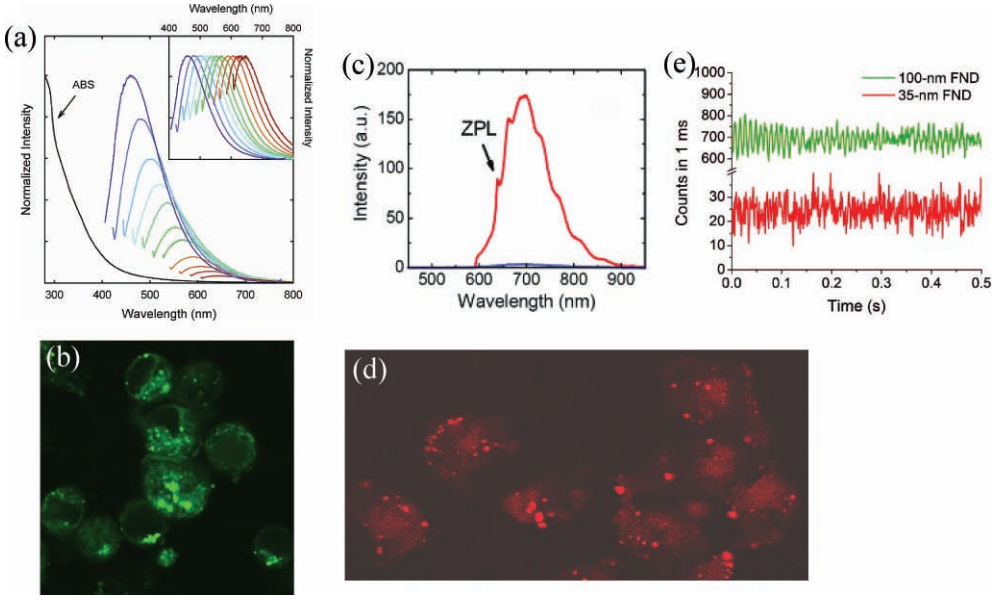

Figure 5. a) The absorption and emission spectra (with progressively longer excitation wavelengths from 400 nm on the left in 20 nm increment, normalized in the inset) of poly(propionylethyleneimine-*co*-ethyleneimine)-passivated carbon dots in an aqueous solution. b) Confocal microscopy image of Caco-2 cells from the uptake experiment with the carbon dots, excited at 488 nm and detected in the 530–750 nm range. Reproduced with permission.[122] Copyright 2006, American Chemical Society. c) Fluorescence spectra of annealed nanodiamonds with (red) or without (blue) proton beam irradiation, excited at 510–560 nm, and collected at a wavelength greater than 590 nm. d) Confocal microscopy image of fluorescent nanodiamond swallowed by 293T human kidney cells about 33 μm in size. The bright red spots are nanodiamonds. Reproduced with permission.[142] Copyright 2005, American Chemical Society. e) Time traces of the fluorescence from single 100-nm (green) or 35-nm (red) fluorescent nanodiamonds acquired with a time resolution of 1 ms, showing a nonblinking behavior. Reproduced with permission.[143] Copyright 2007, National Academy of Sciences (USA).

Ultrasonic electroless treatment grafts HPHT nanodiamonds with aryl groups by using aryl diazonium salts.[121]

4.1.2. Graphite and Complex Carbon Nanoparticles

Luminescent carbon nanoparticles with graphite or more complex structures have been prepared. In contrast to the case of diamond nanoparticles, emissions from these carbon nanoparticles generally stem from surface defects that are either innate or induced by surface treatment.

Laser ablation of a carbon target followed by surface passivation with diamine-terminated oligomeric poly(ethylene glycol) generates 5 nm carbon dots (**Figure 5**a).[122] They show stable photoluminescence without blinking in the visible and near-IR regions with a quantum yield of 4–10%, which can be improved to 45–50% by doping the carbon dots with ZnO or ZnS followed by functionalization with the diamine-polyethylene glycol.[123] Electrochemical treatment of graphite produces carbon nanoparticles with an average diameter of 2 nm that show photoluminescence at 455 and 510 nm.[124,125] Ionic liquid-assisted electrochemical exfoliation of a graphite electrode creates fluorescent 8–10 nm carbon nanoparticles in the graphite structure that exhibit photoluminescence in the 400–600 nm range.[126] Multiwalled carbon nanotubes can be converted electrochemically into carbon nanoparticles with a diameter of 2.8 nm and the materials exhibit 410 nm luminescence.[127] The nanoparticles are graphitic but have an oxidized surface.[128] Carbon nanoparticles can also be derived from candle soot. Oxidative acid treatment of the candle soot produces carbon nanoparticles containing carboxylic acid groups on the surface that emit light in the 415–615 nm range.[129] Two other groups have reported the fabrication of carbon nanoparticles with sizes of 2–6 nm and 4.8 ± 0.6 nm respectively by using nitric acid oxidation of candle soot.[130,131] The materials exhibit photoluminescence at around 520 and 420 nm with quantum yields of 3% and 0.43%, respectively.

The chemical solution route can be utilized to synthesize carbon nanoparticles. Microwave pyrolysis of a mixture of poly(ethylene glycol) and saccharide produces carbon nanoparticles several nanometers in size.[132] They exhibit fluorescence with a peak wavelength of 425–485 nm and a quantum yield of 3.1–6.3%. Thermal decomposition of ammonium citrate salts, or thermal oxidation of an appropriate citrate salt or a preexchanged zeolite host, creates luminescent surface-functionalized carbon nanoparticles with an average size below 10 nm.[133,134] Amorphous carbon nanoparticles with a diameter of 1.5–2.5 nm are prepared from satellite-like carbon/silica composites that are made by using surfactant-modified silica spheres as the carriers and resols as the carbon precursor.[135] The resulting diamine-terminated oligomeric poly(ethylene glycol)-passivated carbon nanoparticles show photoluminescence at 430–580 nm with a quantum yield of 14.7%.

4.2. Biological Applications

Carbon is an environmentally benign element and carbon-based nanoparticles have relatively low cytotoxicity. Furthermore, their surfaces can be functionalized with hydroxyl,

 © 2010 Wiley-VCH Verlag GmbH & Co. KGaA, Weinheim

carboxyl, and amino groups to make them water-soluble and easier to crosslink with biomolecules. Carbon nanoparticles show visible photoluminescence with high efficiency without photobleaching and blinking and are thus very suitable for biological applications such as imaging, diagnostics, and drug delivery.

4.2.1. Conjugation with Biomolecules

Carbon nanoparticles can be conjugated with various biomolecules such as nucleic acids, proteins, and biotins via covalent or noncovalent bonds. This is the first and necessary step in many biological applications. Amino acids can be covalently bonded to small detonation diamond agglomerates after particle surface homogenization by reduction and grafting of a silane linker to form peptides.[136] Aminophenylboronic-acid-functionalized detonation nanodiamond is used to selectively capture glycoproteins from unfractionated protein mixtures.[137] To suppress nonspecific binding with nonglycated proteins, the diamond nanoparticles are first silanized with an alkyl linker chain before linkage with phenylboronic acid to create a shell. Grafting of biotins on detonation nanodiamond has been reported after its surface has been homogenized by borane reduction and functionalized with (3-aminopropyl) trimethoxysilane.[138] The conjugated biotins retain their activity. Conjugation of amino-terminated detonation nanodiamonds to 5-(and-6)-carboxytetramethylrhodamine succinimidyl ester and biotin has been successful and the biotins demonstrate good activity by capturing the streptavidin.[139] The 5 nm nanodiamond obtained by carboxylation/oxidation of diamond in a strong acid followed by coating with poly-L-lysine can be covalently bonded to yeast cytochrome c that possesses a free SH group.[140] The authors have also demonstrated noncovalent adsorption of proteins such as hen-egg white lysozyme onto 100 nm carboxylated/oxidized diamond crystallites and the proteins retain much of the hydrolytic activity afterwards.[141]

4.2.2. Bioimaging

Diamond nanoparticles are efficient biological imaging agents in that they are bright emitters without suffering from photobleaching and blinking. Synthetic type Ib 100 nm diamond nanoparticles containing N-V centers showing fluorescence at 600–800 nm have been utilized in cell imaging (Figure 5c,d).[142] The nanoparticles maintain bright emission after uptake by 293T human kidney cells. They appear to form aggregates within the cell but do not show signs of entering the nucleus. The MTT assays show that addition of up to 400 μg mL^{-1} of nanodiamond does not significantly diminish the cell reduction activity. Diamond particles with a size of 35 nm show no signs of photobleaching after 5 min of continuous excitation.[143] They also exhibit no fluorescence blinking within a time resolution of 1 ms (Figure 5e). The same group reported the fabrication of bright fluorescent 35 nm nanodiamond by helium ion irradiation of synthetic diamond nanoparticles.[144] The resulting nanodiamond allows 3D tracking of single particles within the HeLa cells by use of one- or two-photon excitation. Green fluorescent nanodiamond can also be produced by irradiation of type Ia natural diamond nanocrystallites followed by thermal annealing at 800 °C.[145] The particles show uptake by live HeLa cells. Magnetic and fluorescent water-soluble nanodiamonds are prepared by microwave arcing of a nanodiamond-ferrocene mixture followed by surface grafting with poly(acrylic acids) and fluorescein *o*-methacrylate.[146] They show uptake by HeLa cells. The 35 nm HPHT nanodiamond coated by silanisation or a polyelectrolyte layer is grafted with a fluorescent thiolated peptide via a maleimido function.[147] The resulting conjugates show uptake by Chinese hamster ovary cells and exhibit no cytotoxicity.

Diamond nanoparticles conjugated with biomolecules can be used in specific targeting. Green fluorescent carboxylated nanodiamond electrostatically bound to α-bungarotoxin is linked to the α7-nicotinic acetylcholine receptor located on the cell membrane of oocytes and human lung A549 cancer cells.[148] Blocking of the choline-evoked and receptor-mediated inward currents of the oocytes by nanodiamond-α-bungarotoxin complexes indicates the retained biological activity of α-bungarotoxin. Fluorescent nanodiamond-transferrin bioconjugates are produced by the formation of an amide bond between carboxylated nanodiamond and transferrin and used to target transferrin receptors on HeLa cells.[149] The receptor-mediated uptake of nanodiamond-transferrin into HeLa cells is confirmed. In another work, green fluorescent nanodiamond is attached to antibodies that target intracellular structures such as actin filaments and mitochondria.[150] The actin–antibody coupled nanodiamond conjugates are transfected into HeLa cells mediated by transfection reagents. The mitochondria–antibody conjugated nanodiamonds are first delivered into cells and then selectively targeted to mitochondria. By using both fluorescence and Raman imaging, the visualization of protein-targeted cell interaction is demonstrated by monitoring the carboxylated nanodiamond–lysozyme complex interaction with bacteria Escherichia coli.[151] The resulting nanodiamond–lysozyme complex retains the original functions of the protein. By using growth hormone that has been covalently conjugated to 100 nm carboxylated nanodiamond, the surface growth hormone receptor of A549 human lung epithelial cells can be detected by confocal Raman mapping by detecting the diamond signals.[152]

Carbon nanoparticles with graphite structures can be used in biological imaging with the virtues of tunable emission wavelength and smaller size compared to diamond nanoparticles. However, to date there are only a few reports in this respect. This is because they generally have much lower quantum yields along with much more complex photoluminescence properties that depend sensitively on the fabrication methods compared with the diamond nanoparticles. Recently, the carbon dots produced by laser ablation of carbon targets are used for staining of cells (Figure 5b).[122] By using two-photon excitation in the near-IR, the carbon dots show similar fluorescence relative to one-photon excitation and exploratory results show that it can illuminate human breast cancer cells after internalization.[153] Such carbon dots injected by various ways into living mice remain strongly fluorescent.[154] They are functionalized with the oligomeric PEG and show

 © 2010 Wiley-VCH Verlag GmbH & Co. KGaA, Weinheim

small NANO MICRO

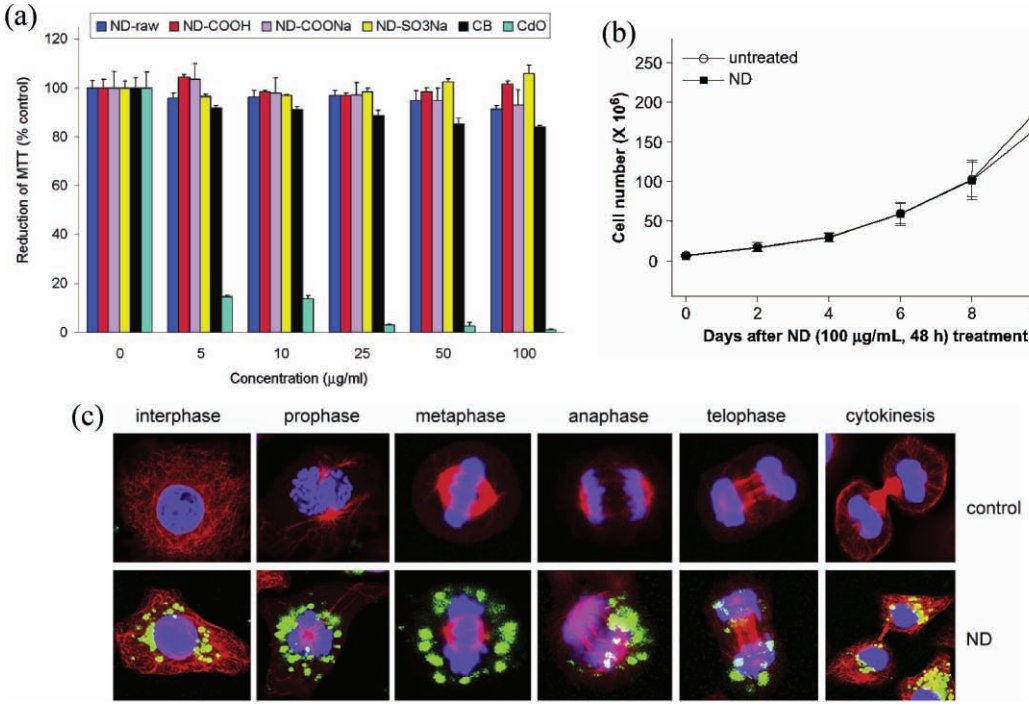

Figure 6. a) Cytotoxicity evaluation of neuroblastoma cells incubated with raw or functionalized nanodiamond (ND), carbon black (CB), and CdO nanoparticles for 24 h by MTT assay. Reproduced with permission.[156] Copyright 2007, American Chemical Society. b) The long-term effect of nanodiamond on the long-term cell growth ability in A549 cells. The cells were treated with or without 100 nm nanodiamond particles (100 μg mL^{-1} for 48 h) and then re-cultured in fresh medium for counting the total cell number by every 2 days. c) The detection and distribution of nanodiamond particles in mitosis examined by laser scanning confocal microscope. A549 cells were incubated with or without 100 μg mL^{-1} nanodiamond particles for 48 h and then re-cultured in fresh medium for 24 h. The microtubule and nuclei were stained and respectively exhibited red and blue colors. The nanodiamonds showed green fluorescence when excited at 488 nm and collected in the range of 510–530 nm. Nanodiamond particles were located in interphase and mitotic phases (prophase, metaphase, and telophase). During cytokinesis, these nanodiamond's particles were separated into two daughter cells. Reproduced with permission.[159] Copyright 2009, Elsevier.

no significant toxic effects to mice despite dosages beyond those commonly used for in vivo optical imaging.[155]

4.2.3. Cytotoxicity

Nanodiamond has excellent biocompatibility. The cytotoxicity of nanodiamond with sizes between 2 and 10 nm has been assessed from the perspective of cell viability such as mitochondrial function and luminescent ATP production.[156] Nanodiamond shows no toxicity to a variety of cell types and does not produce significant reactive oxygen species (ROS) (**Figure 6**a). In experiments comparing the biocompatibility, nanodiamond, carbon nanotubes, and carbon black are separately incubated with neuronal and lung cell lines and the nanodiamond exhibits the best biocompatibility.[157] In comparison with the generation of ROS in cells incubated with carbon nanotubes, no ROS generation is observed from the cells incubated with nanodiamond and the mitochondrial membranes of these cells remain intact. In another comparison experiment, a treatment with 0.1–100 μg mL^{-1} of 5 or 100 nm nanodiamonds neither reduces the cell viability nor alters the protein expression profile in human lung A549 epithelial cells, whereas carbon nanotubes induce cytotoxicity in these cells.[158] Recent work shows that the cell growth ability is not altered by uptake of 100 nm carboxylated nanodiamond after 10 days of cell culture for both A549 lung cancer cells and 3T3-L1 embryonic fibroblasts (Figure 6b,c).[159] The cells retain a single cluster of nanodiamonds in the cytoplasm after sub-culturing for several generations. The diamond nanoparticles do not interfere with the gene or protein expression on the regulation of cell cycle progression and adipogenic differentiation. Another study reveals that the proliferative potential of fluorescent nanodiamond-treated and untreated cells does not exhibit any significant differences when measured at bulk cultures as well as at clonal cell density.[160] The nanodiamond treatment does not affect the in vitro differentiation of 3T3-L1 pre-adipocytes and 489-2 osteoprogenitors. A study of the accumulation location and circulation pathway of 50-nm nanodiamonds shows that the particles predominantly accumulate in the liver after intravenous injection to mice.[161] The spleen and lung are also the target organs. About 60% of the initially digested nanodiamond is trapped in the liver after 0.5 h post dosing and 8% in the lung, and the values remain unchanged even after 28 days. The nanodiamond is barely detectable from the urine and feces.

4.2.4. Uptake Mechanism

To facilitate biological applications, it is essential to understand the cell uptake mechanism of nanoparticles. It has been demonstrated that nanodiamond with a size of 4 or 50 nm is spontaneously swallowed by the living HeLa cells. They are uniformly distributed in the cells and mostly immobilized

 © 2010 Wiley-VCH Verlag GmbH & Co. KGaA, Weinheim

within a few minutes.[162] The 25 nm diamond nanoparticles are observed to enter the HeLa cells and then immobilized in the cell cytoplasm.[163] The low colocalization emission signal ratio between early endosomes and the nanodiamond shows that the nanodiamond is not trapped in endosomes. Receptor-mediated uptake of fluorescent 35- or 140-nm nanodiamond covalently conjugated with folic acid has been observed from HeLa cells.[164] More than 50% of the folic-acid-conjugated nanodiamond particles can be internalized by the cells and after uptake they accumulate in the perinuclear region. Another study shows that luminescent 50 nm nanodiamond enters cells mainly by clathrin-mediated endocytosis.[165] The bigger nanoparticles or aggregates show a higher degree of colocalization with vesicles, whereas the smaller ones appear free in the cytosol. Clathrin-mediated endocytosis of carbon nanoparticles has been proposed by other groups,[159,160] and macropinocytosis is suggested as another possible uptake pathway.[159]

4.2.5. Clinical Applications

Carbon nanoparticles can serve as delivery agents for drugs, genes, and proteins. Structurally ordered mesoporous carbon nanoparticles synthesized using a mesoporous silica nanoparticle as the template exhibit high inhibitory concentration (IC_{50}) values,[166] indicating that these nanoparticles are fairly biocompatible in vitro. They are used to carry the membrane impermeable fluorescence dye Fura-2 to cross the membrane of live HeLa cells and then released inside the cells. The uptake of the Feton-treated triethylammonium-functionalized 4-nm diamond nanoparticles by HeLa cells is observed and some of the nanoparticles are observed to enter the cell nuclei. They can be electrostatically conjugated with plasmid and afterwards cross the HeLa cell membrane, while the plasmid alone cannot cross the membrane.[167]

Nanodiamonds have demonstrated great potential as delivery platforms for various types of therapeutic substances. Acid-treated detonation diamond nanoparticles can form complexes with several kinds of therapeutics including Purvalanol A, 4-hydroxytamoxifen, and dexamethasone via electrostatic interactions.[168] The water solubility of the drugs is improved after forming the complexes. Nanodiamond is shown to ferry doxorubicin hydrochloride (DOX) inside living murine macrophages as well as human colorectal carcinoma cells.[169] Regulation of Cl^- ion concentration controls the adsorption and desorption of DOX (**Figure 7**a). Electrophoretic DNA fragmentation and MTT analysis confirm the functional apoptosis-inducing mechanisms driven by the nanodiamonds-carried DOX. The nanodiamond can be assembled into a closely packed nanodiamond multilayer nanofilm with positively charged poly-L-lysine via the layer-by-layer deposition procedure.[170] Therapeutic molecules are successfully integrated into the film and still preserve their activity. Nanodiamond physically bound to DOX is sandwiched between a base and thin variable layer of parylene C polymer which allows for modulation of release (Figure 7b,c).[171] DOX retains its activity under biological conditions. Nanodiamond functionalized with type I collagen and dexamethasone has also been produced to serve as an active substrate for localized drug delivery.[172] Potent suppressive behavior toward inflammatory gene expression is confirmed indicating the retained activity of the conjugated dexamethasone.

Nanodiamond films can be used in implant coatings. For instance, nanocrystalline diamond films deposited on microscopic glass slides using chemical vapor deposition (CVD) method are oxidized, hydrogenated, and then seeded with human osteoblastlike MG 63 cells.[173] After 7 days, the nanocrystalline diamond films show good adhesion, growth, and maturation of bone-derived cells.

5. Silicon Carbide

5.1. Fabrication and Luminescence Properties

In the mid 1990s, researchers mainly focused on the fabrication and luminescence properties of porous SiC.[174–178]

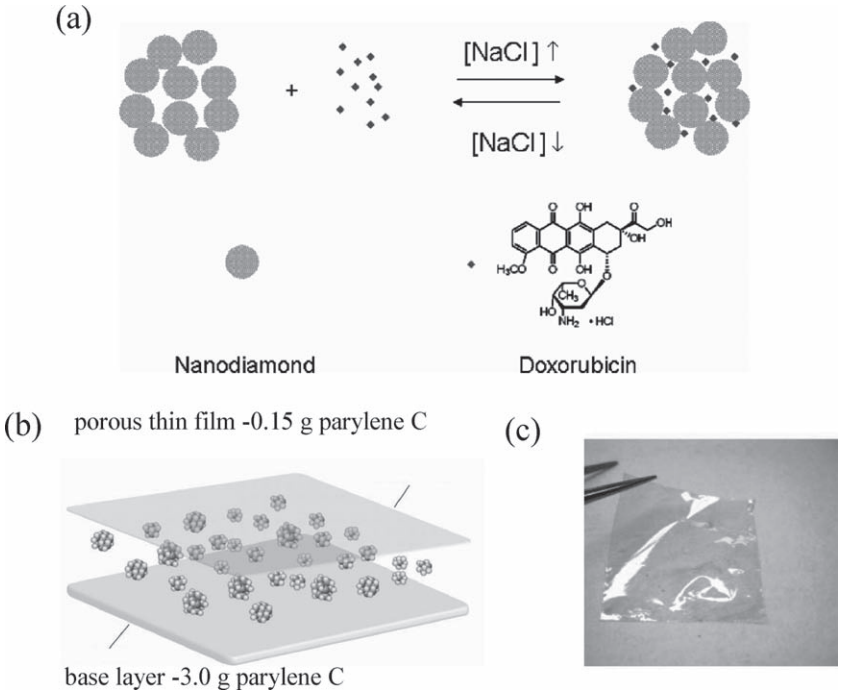

Figure 7. a) Schematic diagram of NaCl-mediated loading and release of doxorubicin hydrochloride. The addition of the salt induces functionalization of the drug onto the nanodiamond aggregate surface. Salt removal drives drug release. Reproduced with permission.[169] Copyright 2007, American Chemical Society. b) Illustrated schematic of hybrid film patch. Nanodiamonds and doxorubicin (DOX) molecules bound through physical interactions in various configurations are deposited atop a base layer of parylene. A final layer of parylene film is then deposited for additional elution control. c) Hybrid film with the patch exhibiting innate flexibility and a thin physical profile. Reproduced with permission.[171] Copyright 2008, American Chemical Society.

© 2010 Wiley-VCH Verlag GmbH & Co. KGaA, Weinheim

NANO MICRO small

In recent years, attention has shifted to the preparation and optical properties of SiC nanoparticles.[178] Compared to Si, only a few methods have been exploited to produce SiC nanoparticles that have sizes small enough to exhibit strong quantum confinement and efficient emissions.

Vapor phase route is employed to synthesize SiC nanocrystallites. Laser pyrolysis of gaseous silane and acetylene produces SiC nanoparticles with sizes ranging from 10 to 25 nm.[179–181] Each nanoparticle is composed of several hexagonal or cubic crystallites with an average diameter of 2.5 nm and embedded in an amorphous SiC matrix. The nanoparticles show red photoluminescence that is supposed to originate mainly from the SiC amorphous fractions of nanopowders and by the Si–O bonds.[179] Hypersonic plasma particle deposition or helicon wave plasma enhanced chemical vapor deposition of vapor-phase $SiCl_4$ (or SiH_4), CH_4, and H_2 precursors yields SiC nanoparticles.[182,183] Pyrolysis of tetramethylsilane and hexamethyldisilazane,[184–186] diethylsilane,[187] or triethylsilane[188] produces crystalline or amorphous SiC nanoparticles with a size of 1–10 nm. Thermal reactions between Na and methylchlorosilane at 1273 K generate SiC nanoparticles with a diameter of 10 nm.[189]

The solution route has been rarely adopted to synthesize SiC nanoparticles. Nanocrystalline 3C-SiC with an average diameter of 25 nm is synthesized by a rapid thermal reduction-carbonization process by using activated carbon and tetrachlorosilane as the sources and Na as the reductant.[190] A similar method produces 3C-SiC hollow nanospheres with diameters of 80-120 nm that are composed of nanoparticles.[191] Carbothermic reaction of SiO_2 xerogel yields powders of SiC particles with a diameter of 10 nm.[192] SiC nanocrystals embedded in a carbon-rich silica matrix with an average diameter of 5–9 nm are prepared from reductive thermal processing of phenylsiloxane polymers achieved by hydrolysis and cocondesation of phenyl trichlorosilane and silicon tetrachloride.[193] Subsequent thermal oxidation followed by HF-etching generates freestanding SiC nanocrystals that show no emissions. A solid-liquid method synthesizes violet emitting 3.5 nm 3C-SiC nanocrystals by laser ablation of silicon wafers in ethanol followed by removal of the mixed Si nanoparticles in HF and H_2O_2.[194]

Electrochemical etching is currently a favorable method to produce luminescent SiC nanocrystals with ultrasmall sizes. Electrochemical etching of polycrystalline 3C-SiC followed by ultrasonic treatment produces 3C-SiC nanocrystals with an average size of 3.9 nm.[195–197] These nanocrystals exhibit robust photoluminescence following the quantum confinement effect with the wavelength tunable from green-yellow to violet at different excitation (**Figure 8**a) and with a quantum yield of 17%.[198] Additionally, the nanocrystals exhibit good water solubility and long-term photostability.[199] 6H-SiC nanocrystals with diameters between 1–8 nm showing UV photoluminescence are prepared by a similar method.[200] Mechanical grinding of electrochemically etched porous 3C- or 6H-SiC layers may also yield luminescent SiC nanocrystals.[201–203] Chemical etching of SiC powders in a mixed solution of HNO_3 and HF produces luminescent 3C-SiC nanocrystals with an average size of 3.6 nm.[204,205]

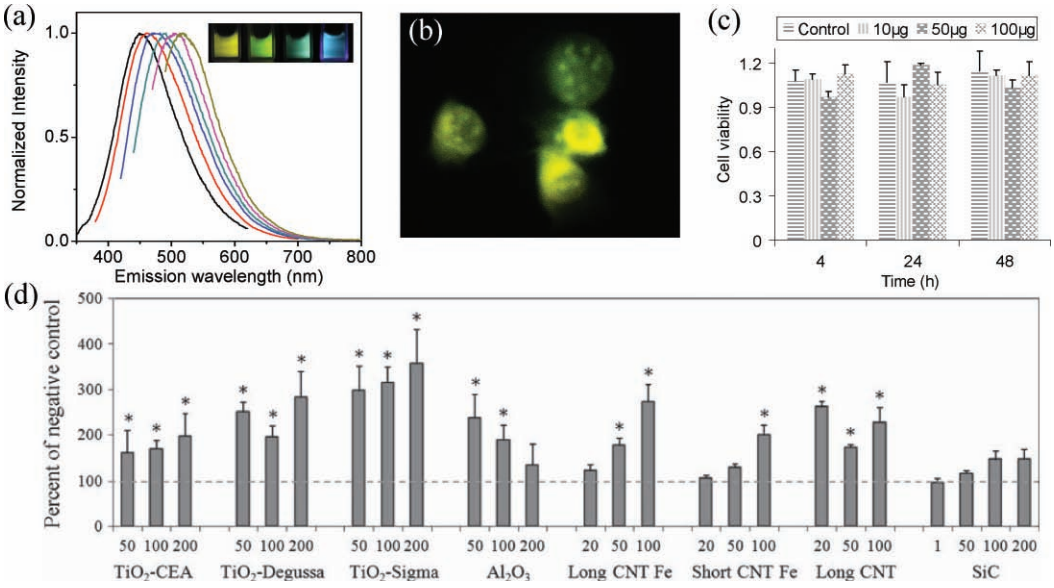

Figure 8. a) Normalized photoluminescence spectra of 3C-SiC nanocrystals in an aqueous solution, excited by the 300, 320, 340, 360, 400, and 440 nm lines of a xenon lamp from left to light. The inset shows the camera images of the aqueous solution of 3C-SiC nanocrystals excited at 450, 430, 410, and 325 nm from left to right by an optical parametric oscillator (OPO). b) Fluorescence microscopy images of hFOB cells after the uptake of 3C-SiC nanocrystals excited at 420–490 nm. Image width: 93 μm. c) Cytotoxicity evaluation of HeLa cells incubated with as-indicated concentrations (per mL) of colloidal 3C-SiC nanocrystals for 4, 24, and 48 h and then analyzed by the standard MTT assay. Error bars indicate the standard deviation for three independent experiments. Reproduced with permission.[198] Copyright 2008, Wiley-VCH. d) Reactive oxide species (ROS) production in NRK-52E cells after incubation with various 1–200 μg mL^{-1} nanoparticles for 24 h. ROS production was evaluated by H2DCF-DA assay. Fluorescence was normalized by total protein content, and expressed as percentage of the negative control, i.e., nonexposed cells. Reproduced with permission.[219] Copyright 2010, Springer.

 © 2010 Wiley-VCH Verlag GmbH & Co. KGaA, Weinheim

There are only few reports on surface functionalization of SiC nanoparticles. Polyacetals have been grafted to SiC nanoparticles with a mean size of 50 nm resulting in improved particle dispersibility in butanone.[206] The unsaturated hydrocarbons on the surface of 3C-SiC nanoparticles 30–50 nm in size react with the radical species generated from azo radical initiators, resulting in surface functionalization of the nanoparticles with carboxyl or amine groups or both groups depending on the types of the employed azo initiators.[207] Polymerization of the conducting polyaniline in the presence of camphorsulfonic acid and SiC nanoparticles results in the formation of polyaniline-camphorsulfonic acid shell with a thickness in the range from 0.5 nm to a few nanometers at the surface of SiC nanocrystals.[208,209]

5.2. Bioimaging

Silicon carbide has long been considered one of the best biocompatible materials. It is light, tough, and chemically inert. It is hence suitable for biomedical implants and coatings. In vitro and in vivo studies have indicated that SiC and hydroxyapatite are equally biocompatible based on particle size for phagocytosis and SiC-coated pins do not inhibit JCRB0603 cell colony outgrowth and react in a manner similar to uncoated titanium pins.[210,211] Carbonization of natural wood at 800–1800 °C in an inert atmosphere followed by infiltration of liquid silicon at 1600 °C generates biomorphic cellular silicon carbide ceramics.[212,213] A combination of excellent mechanical properties and low density renders them good base materials in biomedical devices such as alternative dental and orthopedic implants possessing enhanced mechanical and biochemical properties that ensure optimum fixation to living tissues.[214] Freestanding nanoporous SiC membranes prepared by electrochemical anodization permit diffusion of smaller proteins while excluding larger ones with very low protein adsorption, implying that it is a good semi-permeable material in biomedical applications.[215]

Several preliminary investigations indicate the advantages of using SiC nanoparticles in biological labels. 3C-SiC nanocrystals fabricated by electrochemical etching and ultrasonic treatment possess long-term water solubility and exhibit robust emission with a high quantum yield.[198,199] Together with other favorable intrinsic properties such as small density, high hardness, high thermal conductivity, and high chemical stability, these SiC nanoparticles are good candidates for biological imaging assays. Previous work has indicated that water molecules can easily dissociate at the surface of bulk 3C-SiC giving rise to H- and OH-terminated surfaces,[216,217] which may partially explain the stability of 3C-SiC nanocrystals in water and this property is crucial for long-term biological imaging. Their potential in biological imaging has been demonstrated on hFOB cells (Figure 8b).[198] After uptake by the cells the nanoparticles show also signs of entering the nuclei and they exhibit good resistance against photobleaching. No noticeable cytotoxicity is observed from the 3C-SiC nanocrystals incubated with HeLa cells at a concentration of up to 100 μg mL^{-1} according to the MTT assays (Figure 8c). Imaging of 3T3-L1 fibroblasts with 3C-SiC nanocrystals has also been realized.[218] The cytotoxicity of 17-nm SiC, 12-142 nm TiO_2 nanoparticles, and multi-walled carbon nanotubes to several mammalian cell lines has been compared.[219] The finest TiO_2 nanoparticles are observed to induce the highest cytotoxic effects, while SiC nanoparticles show almost no cytotoxicity (Figure 8d). All the nanoparticles, except SiC nanoparticles, induce reactive oxygen species in the cells.

6. Germanium

6.1. Fabrication and Luminescence Properties

Ge nanoparticles can be synthesized by gas phase methods. Nonthermal plasma dissociation of germanium tetrachloride mixed with hydrogen and argon produces Ge nanocrystals with sizes varying from 4 to 50 nm in the amorphous or crystalline form depending on the plasma power.[220] Subsequent surface functionalization with alkenes renders them dispersible in alkane solvents.[221] Ultrasonic aerosol pyrolysis of tetrapropylgermane produces freestanding Ge nanocrystals with sizes ranging from 3 to 14 nm depending on the tetrapropylgermane concentration.[222]

The solution route proves to be the most successful technique for the synthesis of free Ge nanocrystals. The reaction between NaGe and $GeCl_4$, Mg_2Ge and $SiCl_4$, or NaGe and NH_4Br produces Ge nanocrystals with an average size of 3.5–6.8 nm, and further reaction with lithium alkyl or 1-eicosyne results in alkyl terminated Ge nanocrystals.[223–226] The nanocrystals show emissions across a large portion of the visible region depending on the particles size and surface termination. Butyl-capped Ge nanocrystallites are synthesized by reduction of $GeCl_4$ with Na(naphthalide) and subsequent reaction with butyl Grignard at room temperature.[227] Subsequent anneal at 550-600 °C leads to their transition from amorphous to crystalline phases. The reaction of germanium diiodide with $LiAlH_4$ produces Ge nanocrystals with an average diameter of 3–11 nm depending on the precursor concentration.[228] The reaction between GeO_2 and $NaBH_4$ in an aqueous medium results in 5–20 nm diameter Ge nanoparticles.[229] Ultrasonic solution reduction of $GeCl_4$ by metal hydride and alkaline produces 3–10 nm Ge nanocrystals[230] and borohydride reduction of $GeCl_4$ at room temperature yields 5 nm Ge nanocrystals that emit light at 352 nm.[231]

Inverse micelles have been employed to synthesize Ge nanocrystals. Highly crystalline Ge nanocrystals in the size range of 2–5 nm synthesized by reduction of ionic salts such as $GeCl_4$ in the inverse micelles exhibit photoluminescence in the range 350–700 nm.[232] Ge nanocrystals with an average diameter of 24 nm are synthesized by the reduction of chlorogermaniums with sodium in the inverse micelle solvents using the surfactant $C_{12}E_5$ as a capping agent.[233] Reduction of $GeCl_4$ using strong hydride reducing agents in the reverse micelles produces 5 nm Ge nanocrystals with a narrow size distribution.[234] A subsequent reaction with allylamine renders the nanoparticles hydrophilic and the materials exhibit photoluminescence at 400 nm.

© 2010 Wiley-VCH Verlag GmbH & Co. KGaA, Weinheim

NANO MICRO small

Thermolysis of organometallic Ge is another preparation method. Precipitation in supercritical hexane and octanol with diphenylgermane or tetraethylgermane as the precursors produces Ge nanocrystals with an average diameter of 2–70 nm depending on the reaction temperature and precursor concentration.[235] Such nanoparticles with sizes of 3–4 nm exhibit photoluminescence at 476–536 nm. Thermal decomposition of tetraethylgermane, trichlorogermane, or tetrabutylgermane creates 1–30 nm Ge nanocrystals.[236,237] Visible photoluminescence is observed from those particles smaller than 4 nm. Thermal reduction of $Ge[N(SiMe_3)_2]_2$ generates Ge nanocrystals with an average size of 7 nm and they show photoluminescence at 375–500 nm under different excitation wavelengths.[238] Blue luminescent Ge nanocrystals with an average size of 5.2 nm are fabricated by thermal decomposition of tetra-cis-9-octadecenoic germanium produced by a reaction between $GeCl_4$ and oleylamine.[239] Sulfur-assisted decomposition of triphenylgermanium chloride yields 8 nm Ge nanocrystals that self-assemble into 60 nm nanoclusters after purification.[240]

The sol–gel method can produce Ge nanocrystals encapsulated in the silica matrix. The 5 nm Ge nanocrystals embedded in silica glass are created by hydrolysis of $Si(OC_2H_5)_4$ and $GeCl_4$ followed by heating in hydrogen.[241] The products show strong photoluminescence at 2.32, 2.17, and 2.0 eV. The sol–gel method, in which $Cl_3Ge–C_2H_4–COOH$ serves as the Ge source, yields Ge nanoparticles in silica glass exhibiting strong photoluminescence at 568–775 nm.[242] Violet luminescent oxide-embedded Ge nanocrystals are created by reductive thermal processing of a polymer derived from the hydrolysis and condensation of phenyl trichlorogermane.[243] Freestanding Ge nanocrystals are liberated from the Ge nanocrystals/GeO_2 composite powders by dissolving the oxide matrix in warm water.

The Ge nanocrystals synthesized via the solution route emit light mostly in the visible range and occasionally in the UV range. Colloidal synthesis of IR-emitting 1-octadecene-capped Ge nanocrystals with an average size of 3.2–6.4 nm has been reported by thermal reduction of GeI_2 with *n*-butyllithium (**Figure 9**a).[244] The spectrum peak wavelength increases from 900 to 1400 nm with increasing particle size (Figure 9b) in accordance with the quantum confinement effect. The quantum yield is 8%.

6.2. Bioimaging

Several recent works show the application potential of Ge nanocrystals in biological imaging. Dinitrophenyl-functionalized 3–5 nm Ge nanocrystals prepared from $Ge[\{N(SiMe)_3\}_2]$ are water soluble and exhibit weak fluorescence. After being labeled with carboxyfluorescein, they are cross-linked to immunoglobulin E antibodies on the surface of mast cells RBL-2H3.[245] Incubation of the cells with Ge nanocrystals for 24 h only results in 2% increase in cell death rate compared to dinitrophenyl-functionalized bovine serum albumin. Amine-terminated blue luminescent Ge nanocrystals with an average size of 4.0–5.5 nm are synthesized by hydride reduction of germanium tetrachloride in the inverse micelles

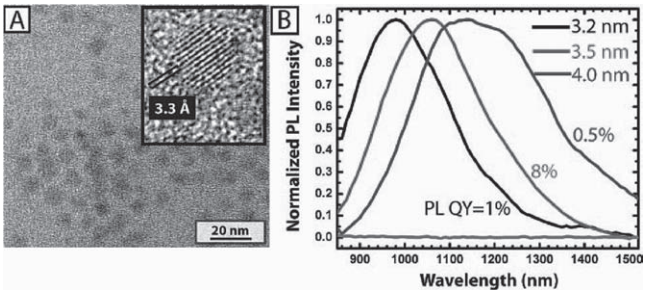

Figure 9. a) TEM image of Ge nanocrystals (4.0 ± 1.7 nm) whose photoluminescence (PL) peak centers at 1160 nm (the most right curve in Figure 9b). The inset shows a high-resolution TEM image of a single Ge nanocrystal. The lattice spacing matches that of the (111) planes of cubic Ge. b) Normalized PL spectra (excited at 808 nm) of 1-octadecene-capped Ge nanocrystals with an average diameter of 3.2, 3.5, and 4.0 nm from left to right. The lower curve shows PL spectrum (not normalized) of trioctylphosphine-capped Ge nanocrystals (3.8 ± 0.8 nm). Reproduced with permission.[244] Copyright 2009, American Chemical Society.

at room temperature followed by surface functionalization with allylamine.[246] Their use in biological imaging is demonstrated by use of HepG2 cells. These nanocrystals show low cytotoxicity according to the mitochondrial activity of the cells.

7. Summary and Outlook

Group IV nanoparticles have emerged as very promising and crucial materials in biological applications such as imaging and drug delivery. They share some virtues and one of them is the favorable biocompatibility. In this respect, diamond and silicon carbide behave rather well. However, before these nanoparticles can be safely used in in vivo biological applications especially when human bodies are involved, a large amount of work is needed to be done to clarify the long-term exposure effect of these nanoparticles to different cells, tissues, and organs. The fluorescence lifetime of group IV nanoparticles generally ranges from several to tens of nanoseconds and hence is suitable for biological imaging assays. Note that some group IV nanoparticles, especially Si nanoparticles, sometimes have luminescence lifetimes on the order of microseconds depending on the fabrication method and luminescence mechanism. The brightness of most fluorescent group IV nanoparticles is high enough to serve as biological labels, among which diamond and Si nanoparticles can have quantum yields close to or even greater than those of group II–VI quantum dots as well as dye molecules. An exception is germanium nanoparticles whose reported luminescence efficiency is relatively low.

On the other hand, each type of group IV nanoparticles has its specific characteristics. For example, silicon carbide and carbon nanoparticles are chemically inert, whereas the surfaces of silicon and germanium nanoparticles are reactive especially in oxygen and humidity environment. Silicon and germanium nanoparticles can be synthesized by various solution methods; in contrast, very few solution methods have been exploited for the synthesis of silicon carbide and carbon

 © 2010 Wiley-VCH Verlag GmbH & Co. KGaA, Weinheim

nanoparticles. Electrochemical etching combined with sonication has been very successful in producing highly luminescent silicon and silicon carbide nanoparticles, but this is not the case for carbon and germanium. In general, the quantum confinement effect is the major luminescence mechanism for silicon, silicon carbide, and germanium nanoparticles, and sometimes surface states may also account for the occurrence of their luminescence. Whereas in diamond nanoparticles, the intentionally created point defects play a key role in generating luminescence.

To enhance the biological applications of group IV nanoparticles, there are several aspects concerning their synthesis and properties that are needed to be seriously considered. First of all, compared to group II–VI quantum dots, the synthesis methods of group IV nanoparticles are not as well established. The solution route has been widely used to synthesize monodisperse group II–VI quantum dots with their sizes and aspect ratio well controlled.[247] An additional virtue of this method lies in the easiness of surface functionalization along with the synthesis process; however, it has been known that group IV nanoparticles have high crystallization temperatures owing to their strong covalent bonding. As a result, the solution-based synthesis route is much more difficult for them. Although there have been a few successes, there are long roads to go before size-controllable monodisperse group IV nanoparticles can be prepared routinely and reproducibly via solution route. There are also difficulties in acquiring narrow emission bands from group IV nanoparticles ascribed to the wide size distribution in these samples. Their emission generally possesses a full width at half maximum (FWHM) of 50–200 nm, and this drawback hampers their wide use in multicolor imaging. Thus many efforts should be made in order to improve the uniformity of nanoparticle sizes so that they can give rise to narrow emission spectra. Group IV nanoparticles are easy to functionalize with a variety of organic ligands, which can improve their water solubility and protect them from potential chemical reactions in physiological environment. However, for chemically inert silicon carbide and diamond nanoparticles, there are difficulties in their surface functionalization and hence more work needs to be done.

Group IV nanomaterials have diverse applications in many areas of nanoscience and nanotechnology. Carbon nanotubes and graphenes are the most important base materials for nanoelectronics.[248,249] Silicon, silicon carbide, and germanium nanocrystals are very efficient and competent light emitters in nanoscale photonics and optoelectronics.[250–252] These aspects combined with their superior biocompatibility render group IV nanoparticles destined to open many new applications in life sciences such as biological labels and diagnostics, drug and biomolecule delivery agents, and bioelectronic devices.

Acknowledgements

This work was supported by the Research Fund for the Doctoral Program of Higher Education (No. 20090092120032) and the Outstanding Young Faculty Grant of SEU (No. 4007021037) as well as City University of Hong Kong Strategic Research Grant (SRG) 7008009.

[1] J. C. Vial, A. Bsiesy, F. Gaspard, R. Hérino, M. Ligeon, F. Muller, R. Romestain, *Phys. Rev. B* **1992**, *45*, 14171.
[2] U. Resch-Genger, M. Grabolle, S. Cavaliere-Jaricot, R. Nitschke, T. Nann, *Nat. Methods* **2008**, *5*, 764.
[3] M. Nirmal, L. Brus, *Acc. Chem. Res.* **1999**, *32*, 407.
[4] T. Pellegrino, S. Kudera, T. Liedl, A. M. Javier, L. Manna, W. J. Parak, *Small* **2005**, *1*, 48.
[5] X. Michalet, F. F. Pinaud, L. A. Bentolila, J. M. Tsay, S. Doose, J. J. Li, G. Sundaresan, A. M. Wu, S. S. Gambhir, S. Weiss, *Science* **2005**, *307*, 538.
[6] D. A. Giljohann, C. A. Mirkin, *Nature* **2009**, *462*, 461.
[7] M. Bruchez Jr., M. Moronne, P. Gin, S. Weiss, A. P. Alivisatos, *Science* **1998**, *281*, 2013.
[8] W. C. W. Chan, S. Nie, *Science* **1998**, *281*, 2016.
[9] C. B. Murray, D. J. Noms, M. G. Bawendi, *J. Am. Chem. Soc.* **1993**, *115*, 8706.
[10] X. Peng, L. Manna, W. Yang, J. Wickham, E. Scher, A. Kadavanich, A. P. Alivisatos, *Nature* **2000**, *404*, 59.
[11] A. M. Derfus, W. C. W. Chan, S. N. Bhatia, *Nano Lett.* **2004**, *4*, 11.
[12] C. Kirchner, T. Liedl, S. Kudera, T. Pellegrino, A. M. Javier, H. E. Gaub, S. Stölzle, N. Fertig, W. J. Parak, *Nano Lett.* **2005**, *5*, 331.
[13] N. Lewinski, V. Colvin, R. Drezek, *Small* **2008**, *4*, 26.
[14] Y. Piao, A. Burns, J. Kim, U. Wiesner, T. Hyeon, *Adv. Funct. Mater.* **2008**, *18*, 3745.
[15] E. Fernandez-Rosas, R. Gómez, E. Ibañez, L. Barrios, M. Duch, J. Esteve, C. Nogués, J. A. Plaza, *Small* **2009**, *5*, 2433.
[16] S. Santavirta, M. Takagi, L. Nordsletten, A. Anttila, R. Lappalainen, Y. T. Konttinen, *Arch. Orthop. Trauma Surg.* **1998**, *118*, 89.
[17] M. Stutzmann, J. A. Garrido, M. Eickhoff, M. S. Brandt, *Phys. Status Solidi A* **2006**, *203*, 3424.
[18] O. Madelung, *Semiconductors: Data Handbook*, 3rd ed., Springer, Berlin, **2004**.
[19] L. T. Canham, *Appl. Phys. Lett.* **1990**, *57*, 1046.
[20] A. G. Cullis, L. T. Canham, P. D. J. Calcott, *J. Appl. Phys.* **1997**, *82*, 909.
[21] O. Bisi, S. Ossicini, L. Pavesi, *Surf. Sci. Rep.* **2000**, *38*, 1.
[22] C. Delerue, G. Allan, M. Lannoo, *Phys. Rev. B* **1993**, *48*, 11024.
[23] M. V. Wolkin, J. Jorne, P. M. Fauchet, G. Allan, C. Delerue, *Phys. Rev. Lett.* **1999**, *82*, 197.
[24] K. Dohnalová, K. Kůsová, I. Pelant, *Appl. Phys. Lett.* **2009**, *94*, 211903.
[25] M. J. Sailor, E. C. Wu, *Adv. Funct. Mater.* **2009**, *19*, 3195.
[26] Z. Yuan, A. Anopchenko, N. Daldosso, R. Guider, D. Navarro-Urrios, A. Pitanti, R. Spano, L. Pavesi, *Proc. IEEE* **2009**, *97*, 1250.
[27] S. Godefroo, M. Hayne, M. Jivanescu, A. Stesmans, M. Zacharias, O. I. Lebedev, G. Van Tendeloo, V. V. Moshchalkov, *Nat. Nanotechnol.* **2008**, *3*, 174.
[28] C. M. Hessel, E. J. Henderson, J. A. Kelly, R. G. Cavell, T. K. Sham, J. G. C. Veinot, *J. Phys. Chem. C* **2008**, *112*, 14247.
[29] M. C. Beard, K. P. Knutsen, P. Yu, J. M. Luther, Q. Song, W. K. Metzger, R. J. Ellingson, A. J. Nozik, *Nano Lett.* **2007**, *7*, 2506.
[30] G. S. He, Q. Zheng, K. T. Yong, F. Erogbogbo, M. T. Swihart, P. N. Prasad, *Nano Lett.* **2008**, *8*, 2688.
[31] J. L. Heinrich, C. L. Curtis, G. M. Credo, K. L. Kavanagh, M. J. Sailor, *Science* **1992**, *255*, 66.
[32] G. Belomoin, J. Therrien, M. Nayfeh, *Appl. Phys. Lett.* **2000**, *77*, 779.

 © 2010 Wiley-VCH Verlag GmbH & Co. KGaA, Weinheim

[33] G. Belomoin, J. Therrien, A. Smith, S. Rao, R. Twesten, S. Chaieb, M. H. Nayfeh, L. Wagner, L. Mitas, *Appl. Phys. Lett.* **2002**, *80*, 841.
[34] D. A. Eckhoff, J. D. B. Sutin, R. M. Clegg, E. Gratton, E. V. Rogozhina, P. V. Braun, *J. Phys. Chem. B* **2005**, *109*, 19786.
[35] J. Valenta, A. Fucikova, I. Pelant, K. Kůsová, K. Dohnalová, A. Aleknavičius, O. Cibulka, A. Fojtík, G. Kada, *New J. Phys.* **2008**, *10*, 073022.
[36] K. A. Littau, P. J. Szajowski, A. J. Muller, A. R. Kortan, L. E. Brus, *J. Phys. Chem.* **1993**, *97*, 1224.
[37] W. L. Wilson, P. F. Szajowski, L. E. Brus, *Science* **1993**, *262*, 1242.
[38] S. Schuppler, S. L. Friedman, M. A. Marcus, D. L. Adler, Y. H. Xie, Y. J. Chabal, T. D. Harris, L. E. Brus, W. L. Brown, E. E. Chaban, P. F. Szajowski, S. B. Christman, P. H. Citrin, *Phys. Rev. B* **1995**, *52*, 4910.
[39] S. H. Tolbert, A. B. Herhold, L. E. Brus, A. P. Alivisatos, *Phys. Rev. Lett.* **1996**, *76*, 4384.
[40] G. Ledoux, J. Gong, F. Huiskena, O. Guillois, C. Reynaud, *Appl. Phys. Lett.* **2002**, *80*, 4834.
[41] X. Li, Y. He, S. S. Talukdar, M. T. Swihart, *Langmuir* **2003**, *19*, 8490.
[42] F. Hua, M. T. Swihart, E. Ruckenstein, *Langmuir* **2005**, *21*, 6054.
[43] R. M. Sankaran, D. Holunga, R. C. Flagan, K. P. Giapis, *Nano Lett.* **2005**, *5*, 537.
[44] H. Takagi, H. Ogawa, Y. Yamazaki, A. Ishizaki, T. Nakagiri, *Appl. Phys. Lett.* **1990**, *56*, 2379.
[45] A. Gupta, M. T. Swihart, H. Wiggers, *Adv. Funct. Mater.* **2009**, *19*, 696.
[46] L. Mangolini, E. Thimsen, U. Kortshagen, *Nano Lett.* **2005**, *5*, 655.
[47] X. D. Pi, R. W. Liptak, J. Deneen Nowak, N. P. Wells, C. B. Carter, S. A. Campbell, U. Kortshagen, *Nanotechnology* **2008**, *19*, 245603.
[48] N. Shirahata, M. R. Linford, S. Furumi, L. Pei, Y. Sakka, R. J. Gates, M. C. Asplund, *Chem. Commun.* **2009**, 4684.
[49] T. van Buuren, L. N. Dinh, L. L. Chase, W. J. Siekhaus, L. J. Terminello, *Phys. Rev. Lett.* **1998**, *80*, 3803.
[50] R. K. Baldwin, K. A. Pettigrew, E. Ratai, M. P. Augustine, S. M. Kauzlarich, *Chem. Commun.* **2002**, 1822.
[51] D. Neiner, H. W. Chiu, S. M. Kauzlarich, *J. Am. Chem. Soc.* **2006**, *128*, 11016.
[52] S. W. Lin, D. H. Chen, *Small* **2009**, *5*, 72.
[53] J. P. Wilcoxon, G. A. Samara, P. N. Provencio, *Phys. Rev. B* **1999**, *60*, 2704.
[54] J. H. Warner, A. Hoshino, K. Yamamoto, R. D. Tilley, *Angew. Chem. Int. Ed.* **2005**, *44*, 4550.
[55] R. D. Tilley, K. Yamamoto, *Adv. Mater.* **2006**, *18*, 2053.
[56] M. Rosso-Vasic, E. Spruijt, B. van Lagen, L. De Cola, H. Zuilhof, *Small* **2008**, *4*, 1835.
[57] N. Shirahata, S. Furumi, Y. Sakka, *J. Cryst. Growth* **2009**, *311*, 634.
[58] J. D. Holmes, K. J. Ziegler, R. C. Doty, L. E. Pell, K. P. Johnston, B. A. Korgel, *J. Am. Chem. Soc.* **2001**, *123*, 3743.
[59] D. S. English, L. E. Pell, Z. Yu, P. F. Barbara, B. A. Korgel, *Nano Lett.* **2002**, *2*, 681.
[60] J. Choi, N. S. Wang, V. Reipa, *Langmuir* **2009**, *25*, 7097.
[61] A. S. Heintz, M. J. Fink, B. S. Mitchell, *Adv. Mater.* **2007**, *19*, 3984.
[62] X. Li, Y. He, M. T. Swihart, *Langmuir* **2004**, *20*, 4720.
[63] R. D. Tilley, J. H. Warner, K. Yamamoto, I. Matsuib, H. Fujimoric, *Chem. Commun.* **2005**, 1833.
[64] F. Hua, F. Erogbogbo, M. T. Swihart, E. Ruckenstein, *Langmuir* **2006**, *22*, 4363.
[65] P. K. Sudeep, Z. Page, T. Emrick, *Chem. Commun.* **2008**, 6126.
[66] C. S. Yang, R. A. Bley, S. M. Kauzlarich, H. W. H. Lee, G. R. Delgado, *J. Am. Chem. Soc.* **1999**, *121*, 5191.
[67] F. A. Reboredo, G. Galli, *J. Phys. Chem. B* **2005**, *109*, 1072.
[68] A. Gali, M. Vörös, D. Rocca, G. T. Zimanyi, G. Galli, *Nano Lett.* **2009**, *9*, 3780.
[69] E. V. Rogozhina, D. A. Eckhoff, E. Grattonb, P. V. Braun, *J. Mater. Chem.* **2006**, *16*, 1421.
[70] S. Sato, M. T. Swihart, *Chem. Mater.* **2006**, *18*, 4083.
[71] R. Guerra, E. Degoli, S. Ossicini, *Phys. Rev. B* **2009**, *80*, 155332.
[72] E. Fernandez-Rosas, R. Gómez, E. Ibañez, L. Barrios, M. Duch, J. Esteve, C. Nogués, J. A. Plaza, *Small* **2009**, *5*, 2433.
[73] R. Gómez -Martínez, P. Vázquez, M. Duch, A. Muriano, D. Pinacho, N. Sanvicens, F. Sánchez-Baeza, P. Boya, E. J. de la Rosa, J. Esteve, T. Suárez, J. A. Plaza, *Small* **2010**, *6*, 499.
[74] D. H. Kim, Y. S. Kim, J. Amsden, B. Panilaitis, D. L. Kaplan, F. G. Omenetto, M. R. Zakin, J. A. Rogers, *Appl. Phys. Lett.* **2009**, *95*, 133701.
[75] D. Jurbergs, E. Rogojina, L. Mangolini, U. Kortshagen, *Appl. Phys. Lett.* **2006**, *88*, 233116.
[76] L. Wang, V. Reipa, J. Blasic, *Bioconjugate Chem.* **2004**, *15*, 409.
[77] J. Choi, N. S. Wang, V. Reipa, *Bioconjugate Chem.* **2008**, *19*, 680.
[78] F. M. Dickinson, T. A. Alsop, N. Al-Sharif, C. E. M. Berger, H. K. Datta, L. Šiller, Y. Chao, E. M. Tuite, A. Houlton, B. R. Horrocks, *Analyst* **2008**, *133*, 1573.
[79] Z. F. Li, E. Ruckenstein, *Nano Lett.* **2004**, *4*, 1463.
[80] Y. He, Z. H. Kang, Q. S. Li, C. H. A. Tsang, C. H. Fan, S. T. Lee, *Angew. Chem. Int. Ed.* **2009**, *48*, 128.
[81] Y. He, Y. Su, X. Yang, Z. Kang, T. Xu, R. Zhang, C. Fan, S. T. Lee *J. Am. Chem. Soc.* **2009**, *131*, 4434.
[82] M. Rosso-Vasic, E. Spruijt, Z. Popović, K. Overgaag, B. van Lagen, B. Grandidier, D. Vanmaekelbergh, D. Domínguez-Gutiérrez, L. De Cola, H. Zuilhof, *J. Mater. Chem.* **2009**, *19*, 5926.
[83] F. Erogbogbo, K. T. Yong, I. Roy, G. Xu, P. N. Prasad, M. T. Swihart, *ACS Nano* **2008**, *2*, 873.
[84] J. W. Aptekar, M. C. Cassidy, A. C. Johnson, R. A. Barton, M. Lee, A. C. Ogier, C. Vo, M. N. Anahtar, Y. Ren, S. N. Bhatia, C. Ramanathan, D. G. Cory, A. L. Hill, R. W. Mair, M. S. Rosen, R. L. Walsworth, C. M. Marcus, *ACS Nano* **2009**, *3*, 4003.
[85] S. Mornet, S. Vasseur, F. Grasset, E. Duguet, *J. Mater. Chem.* **2004**, *14*, 2161.
[86] S. Laurent, D. Forge, M. Port, A. Roch, C. Robic, L. Van der Elst, R. N. Muller, *Chem. Rev.* **2008**, *108*, 2064.
[87] V. Chin, B. E. Collins, M. J. Sailor, S. N. Bhatia, *Adv. Mater.* **2001**, *13*, 1877.
[88] J. Choi, Q. Zhang, V. Reipa, N. S. Wang, M. E. Stratmeyer, V. M. Hitchins, P. L. Goering, *J. Appl. Toxicol.* **2009**, *29*, 52.
[89] K. Fujioka, M. Hiruoka, K. Sato, N. Manabe, R. Miyasaka, S. Hanada, A. Hoshino, R. D. Tilley, Y. Manome, K. Hirakuri, K. Yamamoto, *Nanotechnology* **2008**, *19*, 415102.
[90] A. Fucikova, J. Valenta, I. Pelant, V. Brezina, *Chem. Pap.* **2009**, *63*, 704.
[91] N. H. Alsharif, C. E. M. Berger, S. S. Varanasi, Y. Chao, B. R. Horrocks, H. K. Datta, *Small* **2009**, *5*, 221.
[92] H. Föll, M. Christophersen, J. Carstensen, G. Hasse, *Mat. Sci. Eng. R* **2002**, *39*, 93.
[93] A. B. Foraker, R. J. Walczak, M. H. Cohen, T. A. Boiarski, C. F. Grove, P. W. Swaan, *Pharm. Res.* **2003**, *20*, 110.
[94] J. H. Park, L. Gu, G. von Maltzahn, E. Ruoslahti, S. N. Bhatia, M. J. Sailor, *Nat. Mater.* **2009**, *8*, 331.
[95] J. P. Boudou, P. A. Curmi, F. Jelezko, J. Wrachtrup, P. Aubert, M. Sennour, G. Balasubramanian, R. Reuter, A. Thorel, E. Gaffet, *Nanotechnology* **2009**, *20*, 235602.
[96] Y. Morita, T. Takimoto, H. Yamanaka, K. Kumekawa, S. Morino, S. Aonuma, T. Kimura, N. Komatsu, *Small* **2008**, *4*, 2154.
[97] A. Krüger, F. Kataoka, M. Ozawa, T. Fujino, Y. Suzuki, A. E. Aleksenskii, A. Y. Vuĭ, E. Ōsawa, *Carbon* **2005**, *43*, 1722.
[98] M. Ozawa, M. Inaguma, M. Takahashi, F. Kataoka, A. Krüger, E. Ōsawa, *Adv. Mater.* **2007**, *19*, 1201.

 © 2010 Wiley-VCH Verlag GmbH & Co. KGaA, Weinheim

[99] X. W. Fang, J. D. Mao, E. M. Levin, K. Schmidt-Rohr, *J. Am. Chem. Soc.* **2009**, *131*, 1426.
[100] S. Osswald, G. Yushin, V. Mochalin, S. O. Kucheyev, Y. Gogotsi, *J. Am. Chem. Soc.* **2006**, *128*, 11635.
[101] M. Yeganeh, P. R. Coxon, A. C. Brieva, V. R. Dhanak, L. Šiller, Y. V. Butenko, *Phys. Rev. B* **2007**, *75*, 155404.
[102] C. Kurtsiefer, S. Mayer, P. Zarda, H. Weinfurter, *Phys. Rev. Lett.* **2000**, *85*, 290.
[103] E. Rittweger, K. Y. Han, S. E. Irvine, C. Eggeling, S. W. Hell, *Nat. Photon.* **2009**, *3*, 144.
[104] Y. Y. Hui, Y. R. Chang, T. S. Lim, H. Y. Lee, W. Fann, H. C. Chang, *Appl. Phys. Lett.* **2009**, *94*, 013104.
[105] Y. Sonnefraud, A. Cuche, O. Faklaris, J. P. Boudou, T. Sauvage, J. F. Roch, F. Treussart, S. Huant, *Opt. Lett.* **2008**, *33*, 611.
[106] A. S. Barnard, M. Sternberg, *Diam. Relat. Mater.* **2007**, *16*, 2078.
[107] B. R. Smith, D. W. Inglis, B. Sandnes, J. R. Rabeau, A. V. Zvyagin, D. Gruber, C. J. Noble, R. Vogel, E. Ŏsawa, T. Plakhotnik, *Small* **2009**, *5*, 1649.
[108] J. Tisler, G. Balasubramanian, B. Naydenov, R. Kolesov, B. Grotz, R. Reuter, J. P. Boudou, P. A. Curmi, M. Sennour, A. Thorel, M. Börsch, K. Aulenbacher, R. Erdmann, P. R. Hemmer, F. Jelezko, J. Wrachtrup, *ACS Nano* **2009**, *3*, 1959.
[109] S. Turner, O. I. Lebedev, O. Shenderova, I. I. Vlasov, J. Verbeeck, G. Van Tendeloo, *Adv. Funct. Mater.* **2009**, *19*, 2116.
[110] I. I. Vlasov, O. Shenderova, S. Turner, O. I. Lebedev, A. A. Basov, I. Sildos, M. Rähn, A. A. Shiryaev, G. Van Tendeloo, *Small* **2010**, *6*, 687.
[111] J. R. Rabeau, A. Stacey, A. Rabeau, S. Prawer, F. Jelezko, I. Mirza, J. Wrachtrup, *Nano Lett.* **2007**, *7*, 3433.
[112] I. I. Vlasov, A. S. Barnard, V. G. Ralchenko, O. I. Lebedev, M. V. Kanzyuba, A. V. Saveliev, V. I. Konov, E. Goovaerts, *Adv. Mater.* **2009**, *21*, 808.
[113] J. R. Rabeau, Y. L. Chin, S. Prawer, F. Jelezko, T. Gaebel, J. Wrachtrup, *Appl. Phys. Lett.* **2005**, *86*, 131926.
[114] S. Hu, F. Tian, P. Bai, S. Cao, J. Sun, J. Yang, *Mat. Sci. Eng. B* **2009**, *157*, 11.
[115] S. Hu, J. Sun, X. Du, F. Tian, L. Jiang, *Diam. Relat. Mater.* **2008**, *17*, 142.
[116] S. L. Hu, K. Y. Niu, J. Sun, J. Yang, N. Q. Zhao, X. W. Du, *J. Mater. Chem.* **2009**, *19*, 484.
[117] T. L. Wee, Y. K. Tzeng, C. C. Han, H. C. Chang, W. Fann, J. H. Hsu, K. M. Chen, Y. C. Yu, *J. Phys. Chem. A* **2007**, *111*, 9379.
[118] Y. Liu, Z. Gu, J. L. Margrave, V. N. Khabashesku, *Chem. Mater.* **2004**, *16*, 3924.
[119] W. W. Zheng, Y. H. Hsieh, Y. C. Chiu, S. J. Cai, C. L. Cheng, C. Chen, *J. Mater. Chem.* **2009**, *19*, 8432.
[120] W. S. Yeap, S. Chen, K. P. Loh, *Langmuir* **2009**, *25*, 185.
[121] C. Mangeney, Z. Qin, S. A. Dahoumane, A. Adenier, F. Herbst, J. P. Boudou, J. Pinson, M. M. Chehimi, *Diam. Relat. Mater.* **2008**, *17*, 1881.
[122] Y. P. Sun, B. Zhou, Y. Lin, W. Wang, K. A. S. Fernando, P. Pathak, M. J. Meziani, B. A. Harruff, X. Wang, H. Wang, P. G. Luo, H. Yang, M. E. Kose, B. Chen, L. M. Veca, S. Y. Xie, *J. Am. Chem. Soc.* **2006**, *128*, 7756.
[123] Y. P. Sun, X. Wang, F. Lu, L. Cao, M. J. Meziani, P. G. Luo, L. Gu, L. M. Veca, *J. Phys. Chem. C* **2008**, *112*, 18295.
[124] L. Zheng, Y. Chi, Y. Dong, J. Lin, B. Wang, *J. Am. Chem. Soc.* **2009**, *131*, 4564.
[125] Q. L. Zhao, Z. L. Zhang, B. H. Huang, J. Peng, M. Zhang, D. W. Pang, *Chem. Commun.* **2008**, 5116.
[126] J. Lu, J. Yang, J. Wang, A. Lim, S. Wang, K. P. Loh, *ACS Nano* **2009**, *3*, 2367.
[127] J. Zhou, C. Booker, R. Li, X. Zhou, T. K. Sham, X. Sun, Z. Ding, *J. Am. Chem. Soc.* **2007**, *129*, 744.
[128] J. Zhou, X. Zhou, R. Li, X. Sun, Z. Ding, J. Cutler, T. K. Sham, *Chem. Phys. Lett.* **2009**, *474*, 320.
[129] H. Liu, T. Ye, C. Mao, *Angew. Chem. Int. Ed.* **2007**, *46*, 6473.
[130] S. C. Ray, A. Saha, N. R. Jana, R. Sarkar, *J. Phys. Chem. C* **2009**, *113*, 18546.
[131] L. Tian, D. Ghosh, W. Chen, S. Pradhan, X. Chang, S. Chen, *Chem. Mater.* **2009**, *21*, 2803.
[132] H. Zhu, X. Wang, Y. Li, Z. Wang, F. Yang, X. Yang, *Chem. Commun.* **2009**, 5118.
[133] A. B. Bourlinos, A. Stassinopoulos, D. Anglos, R. Zboril, M. Karakassides, E. P. Giannelis, *Small* **2008**, *4*, 455.
[134] A. B. Bourlinos, A. Stassinopoulos, D. Anglos, R. Zboril, V. Georgakilas, E. P. Giannelis, *Chem. Mater.* **2008**, *20*, 4539.
[135] R. Liu, D. Wu, S. Liu, K. Koynov, W. Knoll, Q. Li, *Angew. Chem. Int. Ed.* **2009**, *48*, 4598.
[136] A. Krüger, Y. Liang, G. Jarre, J. Stegk, *J. Mater. Chem.* **2006**, *16*, 2322.
[137] W. S. Yeap, Y. Y. Tan, K. P. Loh, *Anal. Chem.* **2008**, *80*, 4659.
[138] A. Krueger, J. Stegk, Y. Liang, L. Lu, G. Jarre, *Langmuir* **2008**, *24*, 4200.
[139] S. C. Hens, G. Cunningham, T. Tyler, S. Moseenkov, V. Kuznetsov, O. Shenderova, *Diam. Relat. Mater.* **2008**, *17*, 1858.
[140] L. C. L. Huang, H. C. Chang, *Langmuir* **2004**, *20*, 5879.
[141] T. T. Nguyen, H. C. Chang, V. W. K. Wu, *Diam. Relat. Mater.* **2007**, *16*, 872.
[142] S. J. Yu, M. W. Kang, H. C. Chang, K. M. Chen, Y. C. Yu, *J. Am. Chem. Soc.* **2005**, *127*, 17604.
[143] C. C. Fu, H. Y. Lee, K. Chen, T. S. Lim, H. Y. Wu, P. K. Lin, P. K. Wei, P. H. Tsao, H. C. Chang, W. Fann, *Proc. Natl. Acad. Sci. USA* **2007**, *104*, 727.
[144] Y. R. Chang, H. Y. Lee, K. Chen, C. C. Chang, D. S. Tsai, C. C. Fu, T. S. Lim, Y. K. Tzeng, C. Y. Fang, C. C. Han, H. C. Chang, W. Fann, *Nat. Nanotechnol.* **2008**, *3*, 284.
[145] T. L. Wee, Y. W. Mau, C. Y. Fang, H. L. Hsu, C. C. Han, H. C. Chang, *Diam. Relat. Mater.* **2009**, *18*, 567.
[146] I. P. Chang, K. C. Hwang, C. S. Chiang, *J. Am. Chem. Soc.* **2008**, *130*, 15476.
[147] S. Vial, C. Mansuy, S. Sagan, T. Irinopoulou, F. Burlina, J. Boudou, G. Chassaing, S. Lavielle, *ChemBioChem* **2008**, *9*, 2113.
[148] K. K. Liu, M. F. Chen, P. Y. Chen, T. J. F. Lee, C. L. Cheng, C. C. Chang, Y. P. Ho, J. I. Chao, *Nanotechnology* **2008**, *19*, 205102.
[149] M. F. Weng, S. Y. Chiang, N. S. Wang, H. Niu, *Diam. Relat. Mater.* **2009**, *18*, 587.
[150] M. Mkandawire, A. Pohl, T. Gubarevich, V. Lapina, D. Appelhans, G. Rödel1, W. Pompe, J. Schreiber, J. Opitz, *J. Biophoton.* **2009**, *2*, 596.
[151] J. I. Chao, E. Perevedentseva, P. H. Chung, K. K. Liu, C. Y. Cheng, C. C. Chang, C. L. Cheng, *Biophys. J.* **2007**, *93*, 2199.
[152] C. Y. Cheng, E. Perevedentseva, J. S. Tu, P. H. Chung, C. L. Cheng, K. K. Liu, J. I. Chao, P. H. Chen, C. C. Chang, *Appl. Phys. Lett.* **2007**, *90*, 163903.
[153] L. Cao, X. Wang, M. J. Meziani, F. Lu, H. Wang, P. G. Luo, Y. Lin, B. A. Harruff, L. M. Veca, D. Murray, S. Y. Xie, Y. P. Sun, *J. Am. Chem. Soc.* **2007**, *129*, 11318.
[154] S. T. Yang, L. Cao, P. G. Luo, F. Lu, X. Wang, H. Wang, M. J. Meziani, Y. Liu, G. Qi, Y. P. Sun, *J. Am. Chem. Soc.* **2009**, *131*, 11308.
[155] S. T. Yang, X. Wang, H. Wang, F. Lu, P. G. Luo, L. Cao, M. J. Meziani, J. H. Liu, Y. Liu, M. Chen, Y. Huang, Y. P. Sun, *J. Phys. Chem. C* **2009**, *113*, 18110.
[156] A. M. Schrand, H. Huang, C. Carlson, J. J. Schlager, E. Ŏsawa, S. M. Hussain, L. Dai, *J. Phys. Chem. B* **2007**, *111*, 2.
[157] A. M. Schrand, L. Dai, J. J. Schlager, S. M. Hussain, E. Osawa, *Diam. Relat. Mater.* **2007**, *16*, 2118.
[158] K. K. Liu, C. L. Cheng, C. C. Chang, J. I. Chao, *Nanotechnology* **2007**, *18*, 325102.
[159] K. K. Liu, C. C. Wang, C. L. Cheng, J. I. Chao, *Biomaterials* **2009**, *30*, 4249.

 © 2010 Wiley-VCH Verlag GmbH & Co. KGaA, Weinheim

[160] V. Vaijayanthimala, Y. K. Tzeng, H. C. Chang, C. L. Li, *Nanotechnology* **2009**, *20*, 425103.
[161] Y. Yuan, Y. Chen, J. H. Liu, H. Wang, Y. Liu, *Diam. Relat. Mater.* **2009**, *18*, 95.
[162] F. Neugart, A. Zappe, F. Jelezko, C. Tietz, J. P. Boudou, A. Krueger, J. Wrachtrup, *Nano Lett.* **2007**, *7*, 3588.
[163] O. Faklaris, D. Garrot, V. Joshi, F. Druon, J. Boudou, T. Sauvage, P. Georges, P. A. Curmi, F. Treussart, *Small* **2008**, *4*, 2236.
[164] B. Zhang, Y. Li, C. Y. Fang, C. C. Chang, C. S. Chen, Y. Y. Chen, H. C. Chang, *Small* **2009**, *5*, 2716.
[165] O. Faklaris, V. Joshi, T. Irinopoulou, P. Tauc, M. Sennour, H. Girard, C. Gesset, J. Arnault, A. Thorel, J. Boudou, P. A. Curmi, F. Treussart, *ACS Nano* **2009**, *3*. 3955.
[166] T. W. Kim, P. W. Chung, I. I. Slowing, M. Tsunoda, E. S. Yeung, V. S. Y. Lin, *Nano Lett.* **2008**, *8*, 3724.
[167] R. Martín, M. Álvaro, J. R. Herance, H. García, *ACS Nano* **2010**, *4*, 65.
[168] M. Chen, E. D. Pierstorff, R. Lam, S. Y. Li, H. Huang, E. Osawa, D. Ho, *ACS Nano* **2009**, *3*, 2016.
[169] H. Huang, E. Pierstorff, E. Osawa, D. Ho, *Nano Lett.* **2007**, *7*, 3305.
[170] H. Huang, E. Pierstorff, E. Osawa, D. Ho, *ACS Nano* **2008**, *2*, 203.
[171] R. Lam, M. Chen, E. Pierstorff, H. Huang, E. Osawa, D. Ho, *ACS Nano* **2008**, *2*, 2095.
[172] H. Huang, M. Chen, P. Bruno, R. Lam, E. Robinson, D. Gruen, D. Ho, *J. Phys. Chem. B* **2009**, *113*, 2966.
[173] M. Kopecek, L. Bacakova, J. Vacik, F. Fendrych, V. Vorlicek, I. Kratochvilova, V. Lisa, E. Van Hove, C. Mer, P. Bergonzo, M. Nesladek, *Phys. Status Solidi A* **2008**, *205*, 2146.
[174] T. Matsumoto, J. Takahashi, T. Tamaki, T. Futagi, H. Mimura, Y. Kanemitsu, *Appl. Phys. Lett.* **1994**, *64*, 226.
[175] J. S. Shor, L. Bemis, A. D. Kuttz, I. Grimberg, B. Z. Weiss, M. F. MacMillian, W. J. Choyke, *J. Appl. Phys.* **1994**, *76*, 4045.
[176] O. Konstantinov, A. Henry, C. I. Harris, E. Janzén, *Appl. Phys. Lett.* **1995**, *66*, 2250.
[177] T. L. Rittenhouse, P. W. Bohna, T. K. Hossain, I. Adesida, J. Lindesay, A. Marcus, *J. Appl. Phys.* **2004**, *95*, 490.
[178] J. Y. Fan, X. L. Wu, P. K. Chu, *Prog. Mater. Sci.* **2006**, *51*, 983, and references therein.
[179] A. Kassiba, M. Makowska-Janusik, J. Bouclé, J. F. Bardeau, A. Bulou, N. Herlin-Boime, *Phys. Rev. B* **2002**, *66*, 155317.
[180] J. Bouclé, N. Herlin-Boime, A. Kassiba, *J. Nanopart. Res.* **2005**, *7*, 275.
[181] Y. Kamlag, A. Goossens, I. Colbeck, J. Schoonman, *Appl. Surf. Sci.* **2001**, *184*, 118.
[182] N. P. Rao, N. Tymiak, J. Blum, A. Neuman, H. J. Lee, S. L. Girshick, P. H. McMurry, J. Heberlein, *J. Aerosol Sci.* **1998**, *29*, 707.
[183] W. Yu, W. Lu, Y. Yang, C. Wang, L. Zhang, G. Fu, *Thin Solid Films* **2007**, *515*, 2949.
[184] S. Klein, M. Winterer, H. Hahn, *Chem. Vap. Deposition* **1998**, *4*, 143.
[185] V. Buschmann, S. Klein, H. Fueß, H. Hahn, *J. Cryst. Growth* **1998**, *193*, 335.
[186] H. Lin, J. A. Gerbec, M. Sushchikh, E. W. McFarland, *Nanotechnology* **2008**, *19*, 325601.
[187] T. Rajagopalan, X. Wang, B. Lahlouh, C. Ramkumar, P. Dutta, S. Gangopadhyay, *J. Appl. Phys.* **2003**, *94*, 5252.
[188] V. G. Pol, S. V. Pol, A. Gedanken, *Eur. J. Inorg. Chem.* **2009**, 709.
[189] C. H. Wang, Y. H. Chang, M. Y. Yen, C. W. Peng, C. Y. Lee, H. T. Chiu, *Adv. Mater.* **2005**, *17*, 419.
[190] J. Q. Hu, Q. Y. Lu, K. B Tang, Y. T. Qian, G. E. Zhou, X. M Liu, J. X. Wu, *Chem. Mater.* **1999**, *11*, 2369.
[191] P. Li, L. Xu, Y. Qian, *Cryst. Growth Des.* **2008**, *8*, 2431.
[192] A. Abdel Aal, S. M. El-Sheikh, Y. M. Z. Ahmed, *Mater. Res. Bull.* **2009**, *44*, 151.
[193] E. J. Henderson, J. G. C. Veinot, *J. Am. Chem. Soc.* **2009**, *131*, 809.
[194] S. Yang, W. Cai, H. Zeng, X. Xu, *J. Mater. Chem.* **2009**, *19*, 7119.
[195] X. L. Wu, J. Y. Fan, T. Qiu, X. Yang, G. G. Siu, P. K. Chu, *Phys. Rev. Lett.* **2005**, *94*, 026102.
[196] J. Y. Fan, X. L. Wu, H. X. Li, H. W. Liu, G. G. Siu, P. K. Chu, *Appl. Phys. Lett.* **2006**, *88*, 041909.
[197] J. Y. Fan, H. X. Li, W. N. Cui, *Appl. Phys. Lett.* **2009**, *95*, 021906.
[198] J. Y. Fan, H. X. Li, J. Jiang, L. K. Y. So, Y. W. Lam, P. K. Chu, *Small* **2008**, *4*, 1058.
[199] J. Y. Fan, X. L. Wu, P. Q. Zhao, P. K. Chu, *Phys. Lett. A* **2006**, *360*, 336.
[200] A. M. Rossi, T. E. Murphy, V. Reipa, *Appl. Phys. Lett.* **2008**, *92*, 253112.
[201] J. Botsoa, J. M. Bluet, V. Lysenko, O. Marty, D. Barbier, G. Guillot, *J. Appl. Phys.* **2007**, *102*, 083526.
[202] J. Botsoa, J. M. Bluet, V. Lysenko, L. Sfaxi, Y. Zakharko, O. Marty, G. Guillot, *Phys. Rev. B* **2009**, *80*, 155317.
[203] Y. Zakharko, J. Botsoa, S. Alekseev, V. Lysenko, J. M. Bluet, O. Marty, V. A. Skryshevsky, G. Guillot, *J. Appl. Phys.* **2010**, *107*, 013503.
[204] J. Zhu, Z. Liu, X. L. Wu, L. L. Xu, W. C. Zhang, P. K. Chu, *Nanotechnology* **2007**, *18*, 365603.
[205] X. L. Wu, S. J. Xiong, J. Zhu, J. Wang, J. C. Shen, P. K. Chu, *Nano Lett.* **2009**, *9*, 4053.
[206] J. Che, X. Wang, Y. Xiao, X. Wu, L. Zhou, W. Yuan, *Nanotechnology* **2007**, *18*, 135706.
[207] M. Iijima, H. Kamiya, *J. Phys. Chem. C* **2008**, *112*, 11786.
[208] A. A. Pud, Y. V. Noskov, A. Kassiba, K. Y. Fatyeyeva, N. A. Ogurtsov, M. Makowska-Janusik, W. Bednarski, M. Tabellout, G. S. Shapoval, *J. Phys. Chem. B* **2007**, *111*, 2174.
[209] A. Kassiba, W. Bednarski, A. Pud, N. Errien, M. Makowska-Janusik, L. Laskowski, M. Tabellout, S. Kodjikian, K. Fatyeyeva, N. Ogurtsov, Y. Noskov, *J. Phys. Chem. C* **2007**, *111*, 11544.
[210] P. Aspenberg, A. Anttila, Y. T. Konttinen, R. Lappalainen, S. B. Goodman, L. Nordsletten, S. Santavirtall, *Biomaterials* **1996**, *17*, 807.
[211] S. Santavirta, M. Takagi, L. Nordsletten, A. Anttila, R. Lappalainen, Y. T. Konttinen, *Arch. Orthop. Trauma Surg.* **1998**, *118*, 89.
[212] P. Greil, T. Lifka, A. Kaindl, *J. Eur. Ceram. Soc.* **1998**, *18*, 1961.
[213] P. Greil, T. Lifka, A. Kaindl, *J. Eur. Ceram. Soc.* **1998**, *18*, 1975.
[214] P. González, J. Serra, S. Liste, S. Chiussi, B. León, M. Pérez-Amor, J. Martínez-Fernández, A. R. de Arellano-López, F. M. Varela-Feria, *Biomaterials* **2003**, *24*, 4827.
[215] A. J. Rosenbloom, D. M. Sipe, Y. Shishkin, Y. Ke, R. P. Devaty, W. J. Choyke, *Biomed. Microdevices* **2004**, *6*, 261
[216] F. Amy, Y. J. Chabal, *J. Chem. Phys.* **2003**, *119*, 6201.
[217] G. Cicero, A. Catellani, G. Galli, *Phys. Rev. Lett.* **2004**, *93*, 016102.
[218] J. Botsoa, V. Lysenko, A. Géloën, O. Marty, J. M. Bluet, G. Guillot, *Appl. Phys. Lett.* **2008**, *92*, 173902.
[219] S. Barillet, A. Simon-Deckers, N. Herlin-Boime, M. Mayne-L'Hermite, C. Reynaud, D. Cassio, B. Gouget, M. Carrière, *J. Nanopart. Res.* **2010**, *12*, 61.
[220] R. Gresback, Z. Holman, U. Kortshagen, *Appl. Phys. Lett.* **2007**, *91*, 093119.
[221] Z. C. Holman, U. R. Kortshagen, *Langmuir* **2009**, *25*, 11883.
[222] C. R. Stoldt, M. A. Haag, B. A. Larsen, *Appl. Phys. Lett.* **2008**, *93*, 043125.
[223] B. R. Taylor, S. M. Kauzlarich, *Chem. Mater.* **1998**, *10*, 22.
[224] B. R. Taylor, S. M. Kauzlarich, G. R. Delgado, H. W. H. Lee, *Chem. Mater.* **1999**, *11*, 2493.
[225] C. S. Yang, S. M. Kauzlarich, *Chem. Mater.* **1999**, *11*, 3666.
[226] X. Ma, F. Wu, S. M. Kauzlarich, *J. Solid State Chem.* **2008**, *181*, 1628.
[227] H. W. Chiu, C. N. Chervin, S. M. Kauzlarich, *Chem. Mater.* **2005**, *17*, 4858.

 © 2010 Wiley-VCH Verlag GmbH & Co. KGaA, Weinheim

[228] X. Lu, B. A. Korgel, K. P. Johnston, *Chem. Mater.* **2005**, *17*, 6479.
[229] C. Jing, X. Zang, W. Bai, J. Chu, A. Liu, *Nanotechnology* **2009**, *20*, 505607.
[230] H. P. Wu, J. F. Liu, Y. W. Wang, Y. W. Zeng, J. Z. Jiang, *Mater. Lett.* **2006**, *60*, 986.
[231] N. H. Chou, K. D. Oyler, N. E. Motl, R. E. Schaak, *Chem. Mater.* **2009**, *21*, 4105.
[232] J. P. Wilcoxon, P. P. Provencio, G. A. Samara, *Phys. Rev. B* **2001**, *64*, 035417.
[233] W. Wang, B. Poudel, J. Y. Huang, D. Z. Wang, S. Kunwar, Z. F. Ren, *Nanotechnology* **2005**, *16*, 1126.
[234] J. H. Warner, R. D. Tilley, *Nanotechnology* **2006**, *17*, 3745.
[235] X. Lu, K. J. Ziegler, A. Ghezelbash, K. P. Johnston, B. A. Korgel, *Nano Lett.* **2004**, *4*, 969.
[236] D. Gerion, N. Zaitseva, C. Saw, M. F. Casula, S. Fakra, T. Van Buuren, G. Galli, *Nano Lett.* **2004**, *4*, 597.
[237] N. Zaitseva, Z. R. Dai, C. D. Grant, J. Harper, C. Saw, *Chem. Mater.* **2007**, *19*, 5174.
[238] H. Gerung, S. D. Bunge, T. J. Boyle, C. J. Brinker. S. M. Han, *Chem. Commun.* **2005**, 1914.
[239] H. P. Wu, M. Y. Ge, C. W. Yao, Y. W. Wang, Y. W. Zeng, L. N. Wang, G. Q. Zhang, J. Z. Jiang, *Nanotechnology* **2006**, *17*, 5339.
[240] J. H. Warner, *Nanotechnology* **2006**, *17*, 5613.
[241] M. Nogami, Y. Abe, *Appl. Phys. Lett.* **1994**, *65*, 2545.
[242] H. Yang, X. Wang, H. Shi, S. Xie, F. Wang, X. Gu, X. Yao, *Appl. Phys. Lett.* **2002**, *81*, 5144.
[243] E. J. Henderson, C. M. Hessel, J. G. C. Veinot, *J. Am. Chem. Soc.* **2008**, *130*, 3624.
[244] D. C. Lee, J. M. Pietryga, I. Robel, D. J. Werder, R. D. Schaller, V. I. Klimov, *J. Am. Chem. Soc.* **2009**, *131*, 3436.
[245] T. N. Lambert, N. L. Andrews, H. Gerung, T. J. Boyle, J. M. Oliver, B. S. Wilson, S. M. Han, *Small* **2007**, *3*, 691.
[246] S. Prabakar, A. Shiohara, S. Hanada, K. Fujioka, K. Yamamoto, R. D. Tilley, *Chem. Mater.* **2010**, *22*, 482.
[247] C. Burda, X. Chen, R. Narayanan, M. A. El-Sayed, *Chem. Rev.* **2005**, *105*, 1025.
[248] J. C. Charlier, X. Blase, S. Roche, *Rev. Mod. Phys.* **2007**, *79*, 677.
[249] A. H. Castro Neto, F. Guinea, N. M. R. Peres, K. S. Novoselov, A. K. Geim, *Rev. Mod. Phys.* **2009**, *81*, 109.
[250] O. Boyraz, B. Jalali, *Opt. Express* **2004**, *12*, 5269.
[251] H. Rong, A. Liu, R. Jones, O. Cohen, D. Hak, R. Nicolaescu, A. Fang, M. Paniccia, *Nature* **2005**, *433*, 292.
[252] H. Rong, R. Jones, A. Liu, O. Cohen, D. Hak, A. Fang, M. Paniccia, *Nature* **2005**, *433*, 725.

Received: April 4, 2010
Published online: August 20, 2010

 © 2010 Wiley-VCH Verlag GmbH & Co. KGaA, Weinheim